

# **Response of the Upper Animas River Downstream from Eureka to Discharge of Mill Tailings**

By Kirk R. Vincent and John G. Elliott

Chapter E22 of

**Integrated Investigations of Environmental Effects of Historical  
Mining in the Animas River Watershed, San Juan County, Colorado**

Edited by Stanley E. Church, Paul von Guerard, and Susan E. Finger

Professional Paper 1651

**U.S. Department of the Interior  
U.S. Geological Survey**

# Contents

Abstract.....	893
Introduction and Background.....	893
Purpose and Scope .....	895
Acknowledgments.....	895
Geographic Setting.....	895
Geologic History.....	895
Hydrology .....	897
Flow and Sediment Transport Theory.....	897
Present Condition of Channels and Flood Plains.....	900
Spatial Variation in Geometry .....	900
Channel Conveyance .....	906
Bed Sediment Mobility.....	908
Implications of Channel Patterns.....	909
Sources of Sediment Supplied to the River.....	912
History of Ore Milling.....	912
Other Sources of Sediment.....	914
Photographic Evidence of Change and Recovery.....	914
Early Oblique Photographs.....	914
Aerial Photographs 1945 to 1997 .....	917
Methods.....	917
Results .....	921
Changes Inferred from Flood-Plain Stratigraphy .....	922
Stratigraphy and Sedimentology.....	924
Constraints on Ages of Sediment Deposition .....	925
Stratigraphic Interpretations .....	928
Sediment Chemistry.....	931
Geochemical Methods and Results.....	931
Geochemical Conclusions.....	931
Current Location of Tailings .....	934
Summary and Conclusions.....	936
References Cited.....	938

## Plate

[Plate is on accompanying CD-ROM]

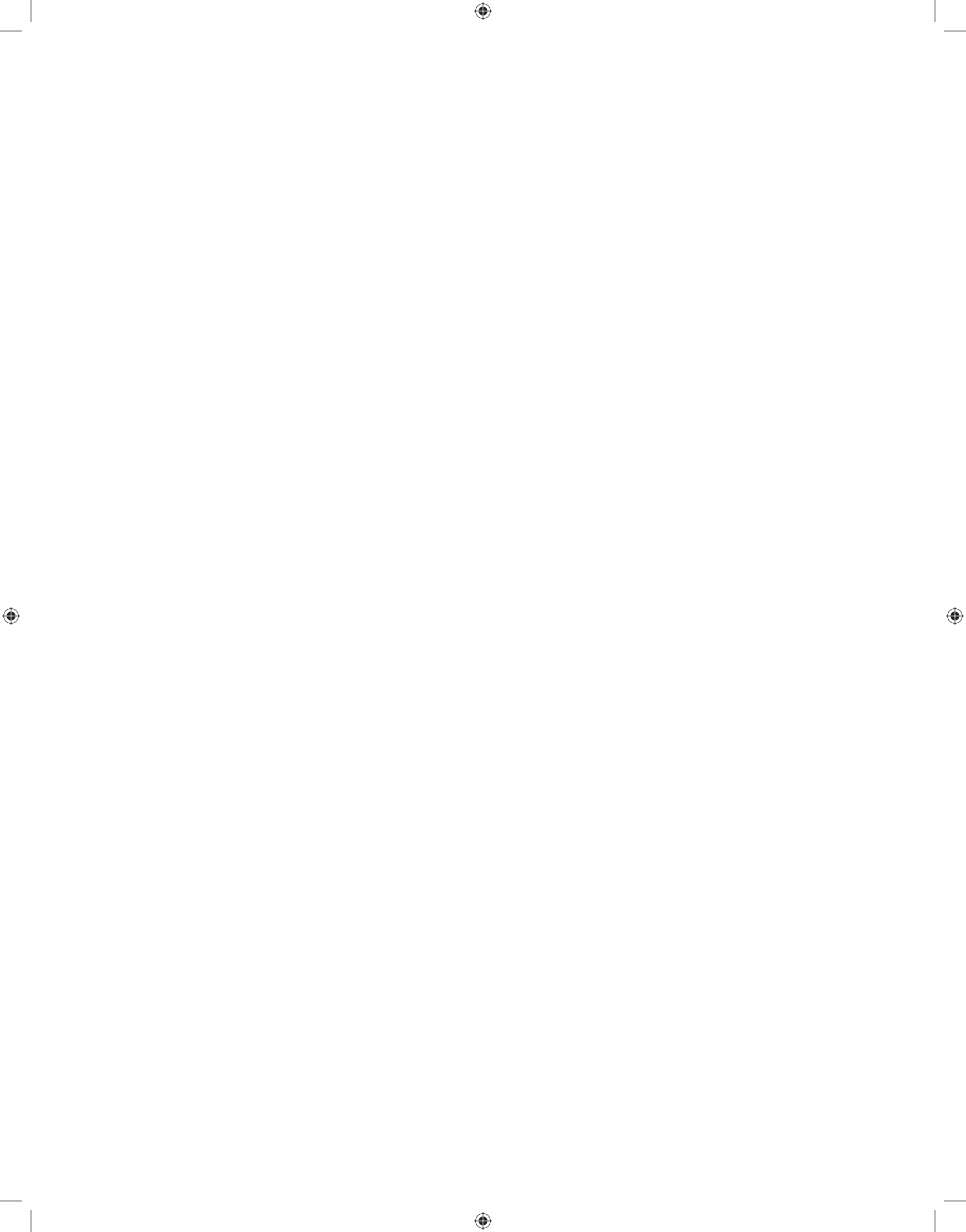
6. [Stratigraphy of late Holocene channel and flood-plain deposits exposed in a trench excavated across the Animas River valley floor 1.4 kilometers downstream of the Eureka townsite, San Juan County, Colorado](#)

## Figures

1.	Location map of upper Animas River study site .....	894
2.	Panoramic photographs of Animas River valley near Eureka, one taken ca 1904 and a repeat photograph taken in 2001 .....	896
3.	Longitudinal profile of upper Animas River valley.....	901
4.	Aerial photographs of study reach, taken in 1951 .....	902
5–7.	Graphs showing:	
5.	Threshold relation between valley slope and bankfull discharge for braided and meandering streams .....	910
6.	Pattern of boundary shear stress for a hypothetical single-thread channel conveying a flow with 2-year recurrence interval.....	911
7.	Combined ore processing rates for the succession of mills in the town of Eureka and in Eureka Gulch.....	912
8.	Etching of photograph taken of Eureka in 1877 .....	915
9–12.	Photographs showing:	
9.	Eureka, and reaches A and B of Animas River, in 1906 and 1999.....	918
10.	Trench section, cemented gravel, and ground-water table below level of stream .....	923
11.	Fresh exposure of flood-plain sediment containing fine-grained tailings, near the trench site .....	926
12.	Willow bush that was repeatedly flood trained and covered by sediment .....	927
13.	Diagram showing summary of dated stratigraphy of the Animas River valley flood plain near the trench site .....	930
14.	Graphs showing concentration of vanadium and zinc in flood-plain sediment.....	932

## Tables

1.	Annual instantaneous peak discharge ( $m^3/s$ ) at streamflow gauging station 09357500 Animas River near Howardsville.....	898
2.	Streamflow characteristics at USGS streamflow gauging station 09357500 Animas River at Howardsville, 1936 through 1982.....	899
3.	Dimensions and other physical characteristics of reaches of the upper Animas River.....	906
4.	Streambed sediment characteristics of the upper Animas River near Eureka.....	907
5.	Statistics from the digital processing and rectification of upper Animas River valley aerial photographs.....	920
6.	Changes in geomorphic and wetland characteristics in reaches of the upper Animas River, from 1945 to 1997 .....	921
7.	Data for radiocarbon samples collected near the trench, downstream of the Eureka townsite.....	929
8.	Concentration of selected elements in deposits of coarse-grained and fine-grained mill tailings .....	933
9.	Spatial extent of surficial fine-grained tailings as interpreted from aerial photographs, by reach and year .....	934
10.	Estimates of volumes and weights of tailings remaining in our study reach .....	936



## **Chapter E22**

# **Response of the Upper Animas River Downstream from Eureka to Discharge of Mill Tailings**

By Kirk R. Vincent and John G. Elliott

### **Abstract**

The Animas River watershed study area in the San Juan Mountains of Colorado was the site of extensive mining and milling during the late 19th and early 20th centuries. We focus on the reach of the Animas River between Howardsville and Eureka, which receives water and sediment from the headwaters area of the upper Animas River. Using geologic mapping, stratigraphic and sedimentological studies of flood-plain sediment, geochronology, historical records, oblique and aerial photographs, sediment transport calculations, and geochemical analysis of sediment, we conclude the following. Prior to mining, the river valley near the eventual town and mill site at Eureka was composed of shallow braided, gravel bedded channels, and multi-thread channels with well-defined banks downstream. The multi-thread channels were located within a silty flood plain consisting of willow thickets and intermittent and localized beaver ponds. A radical change in the stream and flood-plain environment started shortly after A.D. 1900 and concluded downstream of Eureka with aggradation of channels and burial of older sediment with sheets of gravel. This was caused by milling, not mining or other anthropogenic activities. Mills in and near Eureka supplied huge quantities of tailings to the river, at rates 50 to 4,700 times greater than the natural rate of production of sediment from hillslopes prior to mining. The tailings were introduced at a location where the valley profile is strongly concave, where the river is inherently prone to braiding. The introduction of sand-sized tailings altered the bed-load sediment transport regime, and the result was aggradation and stream braiding.

Flood-plain sediment deposited prior to mining has naturally high zinc concentrations close to 1,000 ppm, but the introduction of tailings resulted in an increase of zinc concentrations to more than 4,000 ppm on average and locally to as much as 10,000 ppm. The presence of tailings in stream sediment also increased the concentration of cadmium, copper, lead, and manganese, above the concentrations in prehistorical sediment. Using vanadium as a lithologic tracer for sediment derived from hillslope erosion, we estimate

that the fine fraction of streambed and flood-plain sediment deposited after A.D. 1900 contains, in general, two-thirds tailings and one-third natural sediment. Of the original tailings produced, between 70 and 80 percent has been flushed from the study reach by streamflow, and on the order of 10 percent was mechanically reclaimed and placed in a repository. Of the tailings that remain in the study reach, on the order of 10 percent exists at the surface as easily identifiable tailings beds, but the majority is in the subsurface dispersed within gravel deposits.

### **Introduction and Background**

The portion of the Animas River valley between the abandoned mining towns of Eureka and Howardsville (fig. 1) is important ecologically and in terms of human activities, because it constitutes about 20 percent of the broad and flat ground available in the otherwise rugged San Juan County, Colo. Yet the sediment in this 7-km long reach contains high concentrations of metal, and near Eureka the river is braided and flows across a gravel flood plain devoid of vegetation. As such, that reach is unique in the region. Late 19th and early 20th century hard-rock mining in the watershed (Jones, this volume, Chapter C) created a variety of disturbances. The milling of ore, in particular, resulted in the introduction of large volumes of fine-grained tailings into the fluvial system.

Recent interest in reclamation of inactive mines and river restoration has necessitated identification of contemporary and prehistorical fluvial processes active in the upper Animas River valley, and that is the subject of this chapter. With a better understanding of these processes, strategies designed to address channel instability and contaminant mitigation may have a greater probability of success.

The written record for the area and mining in the area both began in 1871. For that reason the terms prehistorical and premining are synonymous as used herein, and they specifically refer to before A.D. 1871.



## Purpose and Scope

The purpose of this study is to define the late Holocene geomorphic history of the upper Animas River between the abandoned mining towns of Eureka and Howardsville (fig. 1) and identify the important fluvial and anthropogenic processes that resulted in the current condition of the channel and flood plain.

- We present the current physical condition of channels and flood plains, and the contemporary hydrology and sediment transport regime, for comparison with past conditions and potential future conditions.
- We discuss the history of mining and milling in the headwaters area because of the large impact the release of mill tailings has had on the physical and chemical nature of the river channels and flood plain.
- We document how the channels and flood plain have changed over the past 3,000 years, based on the stratigraphy exposed in a trench excavated across the valley floor (pl. 6).
- We document where mill tailings currently reside in and on the flood plain at the trench site, and estimate that for the rest of the reach.
- We compare the historical supply rate of mill tailings with prehistorical supply rates of sediment in order to understand the cause of historical channel change.
- We compare the chemistry of prehistorical and historical sediment in order to understand how the release of mill tailings changed the concentration of metals in stream sediment.
- We document the recovery of the channels and flood plain over the past 50 years, and changes in the locations of tailings, using a time series of aerial photographs.
- Lastly we discuss constraints on future efforts to mitigate contamination caused by the presence of mill tailings, and constraints on future efforts to reconfigure the stream channels in the study area.

This chapter also serves as an example for future work in other areas. We demonstrate the consequences of the introduction of mill tailings into the environment that should be expected in other mining areas, and how to identify those consequences. We also demonstrate how the results of numerous geomorphological methods can be integrated into an understanding of the configuration of stream channels as they were prior to disturbance, and an understanding of the constraints on future channel configuration. At the national level, projects aimed at “restoring” disturbed channels have typically proceeded without that basic understanding.

## Acknowledgments

The U.S. Bureau of Land Management funded the trenching and other aspects of our work; we acknowledge Stephanie O’Dell and Rob Robinson for that funding. The trench (pl. 6) was excavated using a trackhoe operated by Bill Simon. The mineralogy of coarse-grained tailings observed in the trench was corroborated by Steve Fearn. Mike Scott interpreted the growth rings of the willow shown in figure 12. Stevan Gyetvai rectified and registered the aerial photographs from GPS data, and computed channel lengths and valley floor and wetland areas with GIS techniques. Jonathan Evans assisted with channel surveys and streambed-sediment measurements. Rob Robinson, and in particular J. Dungan Smith provided many constructive comments on the manuscript.

## Geographic Setting

This chapter documents the nature and history of landforms along 7 km of the upper Animas River between the abandoned mining towns of Eureka and Howardsville (fig. 1). The Animas River originates in subalpine valleys of the San Juan Mountains of San Juan County, Colo., flows southwest through the study reach (fig. 2), ultimately passes the towns of Silverton and Durango, and joins the San Juan River at Farmington, N. Mex. In the study area, the valley floor is at altitude of 2,970 m, but the surrounding hillslopes extend up to 4,111 m. Those hillslopes are dominated by exposed bedrock and tundra vegetation above the timberline (at about 3,600 m), and are dominated by Engelmann spruce below the timberline. In the valley bottom, spruce forest and open grasslands dominate alluvial fans. Stream terraces and flood plains either are devoid of vegetation (fig. 2) or support thickets of bog birch and willow, sedge wetlands, and spruce forests.

## Geologic History

The bedrock geology, and the mineralization that made the area famous, are discussed by Yager and Bove (this volume, Chapter E1 and pl. 1) and Bove and others (this volume, Chapter E3). For our chapter the salient aspect of the bedrock geology is that it is composed of erosion-resistant volcanic rock. Thus talus fields are common, hillslope soils are thin and fragmental, and alluvial deposits are coarse and contain little silt and clay. The latest Quaternary geologic history of the region has been presented by Blair and others (2002) and Vincent and others (this volume, Chapter E16), and we add to that knowledge base. Atwood and Mather (1932) developed the original maps showing the extent of latest Pleistocene glaciation in the San Juan region. Alpine glaciers occupied the Animas River valley, and the subsequent action of streams is superimposed on that glacial terrain. Few if any surficial deposits predate the last glaciation. Although numerous rock glaciers are scattered through the San Juan Mountains, there is no evidence of glaciation at



**Figure 2.** Panoramic photographs of Animas River valley near Eureka; mouth of Eureka Gulch visible right of center and Howardsville just out of sight down valley on extreme left. In center of photographs, view looks west. Upper photograph (A) was taken by an unknown photographer in or before 1904 and was published by the *Silverton Standard* (1904). It is provided here courtesy of William Jones. Note buildings of Sunnyside Mill # 2 (AMLI site # 165) and town of Eureka right of center and Silverton Northern train in center foreground. Lower photographic mosaic (B) was taken in 2001 by Kirk Vincent. Our reach B dominates the photograph, and lower portion of reach A is visible on far right. Dashed line and T, location of trench (pl. 6).

any time during the Holocene. Whether by glacial erosion or stream erosion, bedrock became exposed in the valley bottom upstream of Eureka forming a waterfall. The exposed bedrock controls the base level for the river upstream and causes a steep, concave slope in the valley below—at the head of the study area. During the Holocene, tributary streams have shed sediment into the valley, forming alluvial fans, which the Animas River has not been able to remove. In our study area (fig. 1), tributary streams enter the valley from the northwest and southeast in opposition to one another, and the largest fans occur at the mouths of Minnie and Maggie Gulches and Cunningham Creek. As a result the Animas River flood plain consists of three wide reaches, with intervening reaches where the river (with little or no flood plain) passes between pairs of encroaching fans (fig. 1). Perhaps only a fraction of each fan is active at present. The wide flood-plain reaches have been aggrading slowly for at least the last 3,000 years. That and other aspects of the late Holocene geomorphic history are developed herein.

## Hydrology

Precipitation in the area is predominantly snowfall, but rain is delivered in the summer by thunderstorms and by Pacific tropical storms in the fall. The Silverton weather station records mean annual temperature of 1.7°C and mean annual precipitation of 61 cm (National Weather Service data), but precipitation is about twice that in the surrounding mountains (von Guerard and others, this volume, Chapter B). The upper Animas River is a snowmelt-dominated stream with annual peak discharge usually occurring from late May through June (table 1), but intense rainfall in the late summer has produced large floods (Pruess, 1996). Streamflow data (table 1) are available for the gauging station on the Animas River at Howardsville (09357500), which was operated by the USGS from 1936 to 1982 and by the Colorado State Engineer since 1983. The drainage area upstream from the gauge is 145 km<sup>2</sup>. Annual peak discharges vary widely in magnitude and reflect the water content of the preceding winter snowpack and the spring weather patterns.

Annual floods recorded at station 09357500 have ranged from 12.9 m<sup>3</sup>/s in 1977 to 56.1 m<sup>3</sup>/s in 1949 (table 1). Other large floods were observed in the upper Animas River valley, prior to establishment of the stream gauge, specifically in 1927, 1921, and 1911. A streamflow gauging station on the Animas River at Durango, Colo., about 80 km downstream from Howardsville, recorded a peak discharge of 570 m<sup>3</sup>/s in 1927. A regression between the annual peak discharge at the Howardsville gauge and the peak discharge at the Durango gauge resulted in a relatively poor coefficient of determination ( $R^2 = 0.69$ ); however, the data from the gauge at Durango suggest that the 1927 flood at Howardsville may have been larger than any recorded since 1936 (the year that the USGS began gathering streamflow data at Howardsville).

Oblique photographs in the San Juan County, Colo., Court House collection show two Howardsville bridges washed out by flooding in 1921. A tropical storm on October 5, 1911 (Pruess, 1996) resulted in extreme flooding and damage in the watershed (Durango Evening Herald, 1911). The discharge of the 1911 flood was probably extreme in the study reach, because the site (Gladstone) where the most intense rainfall was recorded (21 cm of rainfall in a 24-hour period) is located 8 km northwest of Howardsville. USGS historical background observations indicate that the 1911 flood at Howardsville was the “greatest flood since at least 1885.” Although the discharges for these historical floods are not known, the events are important in that they occurred during or just after the period of the largest introduction of sand-sized mill tailings to the fluvial system in the reach of concern in this chapter.

Hydrologic characteristics of the upper Animas River valley were determined using data for the Howardsville stream gauge (table 1) from 1936 through 1982, the period for which the gauge was operated by the USGS. Flood frequency and the duration of daily mean discharges were calculated by standard USGS procedures (U.S. Interagency Advisory Committee on Water Data, 1982). A flood recurrence interval is a statistical expression based on a long flood series. At the Howardsville gauge, an annual peak discharge of 56.8 m<sup>3</sup>/s is thought to be equaled or exceeded every 100 years, and the discharge of 41.3 m<sup>3</sup>/s has a recurrence interval of 10 years (table 1). Floods with recurrence interval greater than 10 years occurred eight times since the stream gauge was established: in 1938, 1949, 1952, 1953, 1957, 1973, 1985, and 1995. Only one flood (1949) with recurrence interval greater than 50 years occurred since 1936. The annual peak flow with 2-year recurrence interval has magnitude of 27.7 m<sup>3</sup>/s. This discharge, as an instantaneous annual flood peak, was equaled or exceeded in 32 years from 1936 to 1998 (table 1). As a daily mean discharge (table 2), 27.7 m<sup>3</sup>/s was equaled or exceeded approximately 0.14 percent of the time on average, or on less than one day per year.

## Flow and Sediment Transport Theory

In this chapter we make several discharge and sediment transport calculations in order to explore why the Animas River is locally braided, and in order to understand the general magnitude of flow events required to mobilize the streambed and certain tailings deposits. To be concise we present in this section all of the transport equations used in the chapter. The flow equations presented are appropriate for turbulent water flows that are steady and horizontally uniform, which can be approximated in a complicated geometric situation by reach averaging. Where appropriate we note the value of constants in parentheses.

We calculate the discharge conveyed by select channels using the following relationships. By definition the volumetric rate of flow, discharge ( $Q$ ), equals the cross-sectional area ( $A$ )

**Table 1.** Annual instantaneous peak discharges (m<sup>3</sup>/s) at streamflow gauging station 09357500 Animas River near Howardsville.

[Discharges were measured in ft<sup>3</sup>/s and were converted using m<sup>3</sup>/s = ft<sup>3</sup>/s \* 0.028317 rounded to the nearest whole number. Noted in parentheses are floods known from anecdotal evidence, and the position in the time series of aerial photographs used by this study]

Year	Month	Discharge	Year	Month	Discharge
1885	(unknown)	(large flood)	1964	May	24
			1965	June	33
1911	Oct.	(large flood)	1966	May	20
			1967	May	27
1921	(unknown)	(flood)	1968	June	35
			1969	May	21
1927	June	(large flood)	1970	Sept.	33
			1971	June	23
1936	May	24	1972	June	23
1937	May	25	1973	June	43
1938	June	48	1973	Sept.	(photograph)
1939	June	19	1974	May	18
1940	May	23	1975	July	38
1941	June	31	1976	June	23
1942	June	30	1977	June	13
1943	June	20	1978	June	34
1944	June	32	1979	June	32
1945	June	27	1980	June	34
1945	Oct.	(photograph)	1981	June	28
1946	June	30	1982	June	27
1947	June	32	1983	June	34
1948	June	34	1984	May	31
1949	June	56	1985	June	49
1950	June	22	1986	June	36
1951	June	24	1987	June	23
1951	Sept.	(photograph)	1987	Sept.	(photograph)
1952	June	43	1988	June	22
1953	June	46	1989	May	16
1954	May	15	1990	June	27
1955	June	30	1991	June	24
1956	May	26	1992	June	16
1957	June	48	1993	June	28
1958	June	32	1994	June	37
1959	June	24	1995	July	43
1960	June	34	1996	May	31
1960	August	(photograph)	1997	June	41
1961	May	23	1997	October	(photograph)
1962	June	23	1998	June	23
1963	May	18			

times the mean velocity (*U*) of the flow. In a steady, horizontally uniform flow the reach-averaged mean flow velocity can be calculated using

$$U = (u^*/k) [\ln(h/z_o) - 0.74] \tag{1}$$

where

- u\** is the shear velocity (defined in equation 2),
- k* is von Karman's constant (0.408),
- h* is the reach-averaged flow depth,

and

- z<sub>o</sub>* is a parameter related to the reach-averaged channel roughness.

Because the channels in question are gravel bedded, we assume that *z<sub>o</sub>* is equivalent to 0.1 \* *D<sub>84</sub>* (Whiting and Dietrich, 1989) where *D<sub>84</sub>* is the 84th percentile of the bed-sediment size distribution. Owing to bed and channel irregularities *z<sub>o</sub>* might be as much as three times this value. The equation assumes a quasi-logarithmic velocity profile (Wiberg and Smith, 1991). In our application we ignore bank effects because the channels are wide compared to their depths. For that reason we estimated the reach-averaged cross-sectional shape to be that of the surveyed cross sections, and then we subdivided the cross sections into short width-increments of uniform depth. Discharge was calculated for each increment

**Table 2.** Streamflow characteristics at USGS streamflow gauging station 09357500 Animas River at Howardsville, 1936 through 1982.

[Recurrence interval in years equals the reciprocal of exceedence probability (streamflow duration in percentage of time specific discharge is equaled or exceeded)]

Peak flow frequency		Daily discharge	
Recurrence interval (years)	Discharge (m <sup>3</sup> /s)	Equaled or exceeded (percent time)	Discharge (m <sup>3</sup> /s)
1.05	16.5	95	0.371
1.11	18.5	90	0.413
1.25	21.3	85	0.444
2.00	27.7	80	0.475
5	36.0	75	0.507
10	41.3	70	0.538
25	47.7	65	0.591
50	52.3	60	0.654
100	56.8	55	0.741
200	61.3	50	0.869
500	67.2	45	1.01
		40	1.24
		35	1.58
		30	2.08
		25	2.87
		20	4.05
		15	6.06
		10	8.98
		5	13.5

using equation 1 and the appropriate increment-area, and then summed to obtain the total discharge. For rivers with the morphology of the Animas River in the upper part of our study area, this procedure is accurate (J. Dungan Smith, oral comm., 2004). In equation 1 the shear velocity is

$$u^* = (ghS)^{1/2} \tag{2}$$

where

- $g$  is the acceleration due to gravity (9.8 m/s<sup>2</sup>),
- $h$  is again the reach-averaged flow depth,

and

- $S$  is the reach-averaged slope of the riverbed.

Technically  $S$  is the sine of the slope (slope in degrees), but we substituted the tangent (rise over run) into the equation. In this application where the slopes are close to 1/2°, that substitution results in an insignificant error (0.005 percent).

Sedimentary particles on a riverbed begin to move when the local boundary shear stress ( $\tau_b$ ), approximated here by the reach-averaged value, exceeds a critical value ( $\tau_c$ ) that depends on sediment and fluid parameters. In a steady, horizontally uniform flow the boundary shear stress is

$$\tau_b = \rho ghS \tag{3}$$

where

- $\rho$  is the fluid density (1,000 kg/m<sup>3</sup>).

The critical shear stress for initiation of motion was first evaluated by Shields (1936) and now forms the basis for sediment transport calculations. For its application see Henderson (1966), Graf (1971), or Middleton and Southard (1984). In general, the critical shear stress can be calculated by estimating what is known as the critical Shields' stress or Shields' parameter ( $\tau_c$ ) and using

$$\tau_c = (\tau_c)_c [(\rho_s - \rho)gD] \tag{4}$$

where

- $\rho_s$  is the sediment density (assumed to be 2,700 kg/ m<sup>3</sup>)

and

- $D$  is the particle size of interest.

Although the Shields method can be applied to individual grains in a poorly sorted sediment (Wiberg and Smith, 1987), it is usually used to calculate the initial motion of the entire mixture and for this purpose the median diameter ( $D_{50}$ ) of the sediment distribution is used (Wilcock, 1992, p. 297).

The crux of the problem is in evaluating the Shields parameter (Elliott and Hammack, 2000; Komar, 1987; Wiberg and Smith, 1987; Andrews, 1983; Parker and others, 1982; Neill, 1968). The Shields parameter depends on the geometric properties of the sediment grains (including shape and angularity), on the pockets within which the sediment particles rest (which depend on the shape, angularity, and sorting of the bed material), on any cohesive forces among sediment grains, and on the particle Reynolds number. For the flows of interest here and materials of pebble and larger size, however, the dependence of the Shields parameter on cohesive forces and on the particle Reynolds number disappears, but the dependence on the geometric properties of the grains and the bed becomes very strong. For elliptical-shaped coarse sediment, significant motion occurs when the Shields parameter is approximately 0.06 (Wilcock and McArdell, 1993; Wiberg and Smith, 1987). For smoother, more spherical clasts, this value is smaller. In addition, the original Shields relation was generated for significant motion. The first motion of pebbles and cobbles usually occurs at a substantially lower value of the Shields parameter because the first clasts to move are those resting in favorable pockets in the bed (Lisle and others, 1993; Andrews and Smith, 1992; Milhous, 1982). As a compromise when Shields' approach is used for first motion of coarse materials, this asymptotic value is usually reduced to 0.03 or less. We use 0.03 as the value of the Shields parameter in our calculations of initiation of first motion, and we use 0.06 as the value of the Shields parameter in our calculations of significant motion.

We discuss sites where the bed material  $D_{50}$  is 39 mm and 110 mm (table 4), in the sections titled "Channel Conveyance" and "Bed Sediment Mobility." Using equation 4 and the assumptions made herein, we calculated the critical shear stress for initiation of motion of those materials to be 19.5

and 55 N/m<sup>2</sup>, respectively. The shear stress for significant motion of those materials is 39 and 110 N/m<sup>2</sup> (Newtons per square meter), respectively.

The bed load transport of gravel can be calculated using the equation of Meyer-Peter and Müller (1948), which in essence is an expression of the boundary shear stress in excess of the critical shear stress. Again, for its application see Henderson (1966), Graf (1971), or Middleton and Southard (1984). Just as critical shear stress is scaled by the Shields parameter (equation 4), the relation uses what is called the Shields stress

$$(\tau_*)_b = \tau_b / [(\rho_s - \rho)gD] \quad (5)$$

which is a function of boundary shear stress (equation 3). For the sediment-volume transport rate per unit channel width ( $Q_s$ ), equation 5 can be formulated as

$$Q_s = (8[(\tau_*)_b - (\tau_*)_c]^{1.5}) * ([\rho' gD^3]^{0.5}) \quad (6)$$

where the sediment/fluid density contrast is expressed as the fraction  $\rho' = (\rho_s - \rho)/\rho$ .

We use equation 6 to calculate sediment transport for several types of channels present in the landscape, in the section titled, "Bed Sediment Mobility." We also calculate sediment transport for a hypothetical single-thread channel, and estimate the magnitude of sediment deposition by comparing changes in  $Q_s$  moving in the downstream direction, in the latter half of the section titled, "Implications of Channel Patterns."

## Present Condition of Channels and Flood Plains

We start our analysis by discussing the general planimetric and large-scale geomorphic characteristics of the upper Animas River and the flood plain as it was in the latter half of the 20th century. We utilized topographic maps, aerial photographs taken between 1945 and 1997, and onsite measurements made in 1998. The discussion is illustrated using (1) a longitudinal profile of the valley (fig. 3) constructed using the 1955 USGS 1:24,000 quadrangle maps, which have contour interval of approximately 13 m (40 feet); (2) aerial photographs taken in 1951 (fig. 4); and (3) data derived from those sources (table 3).

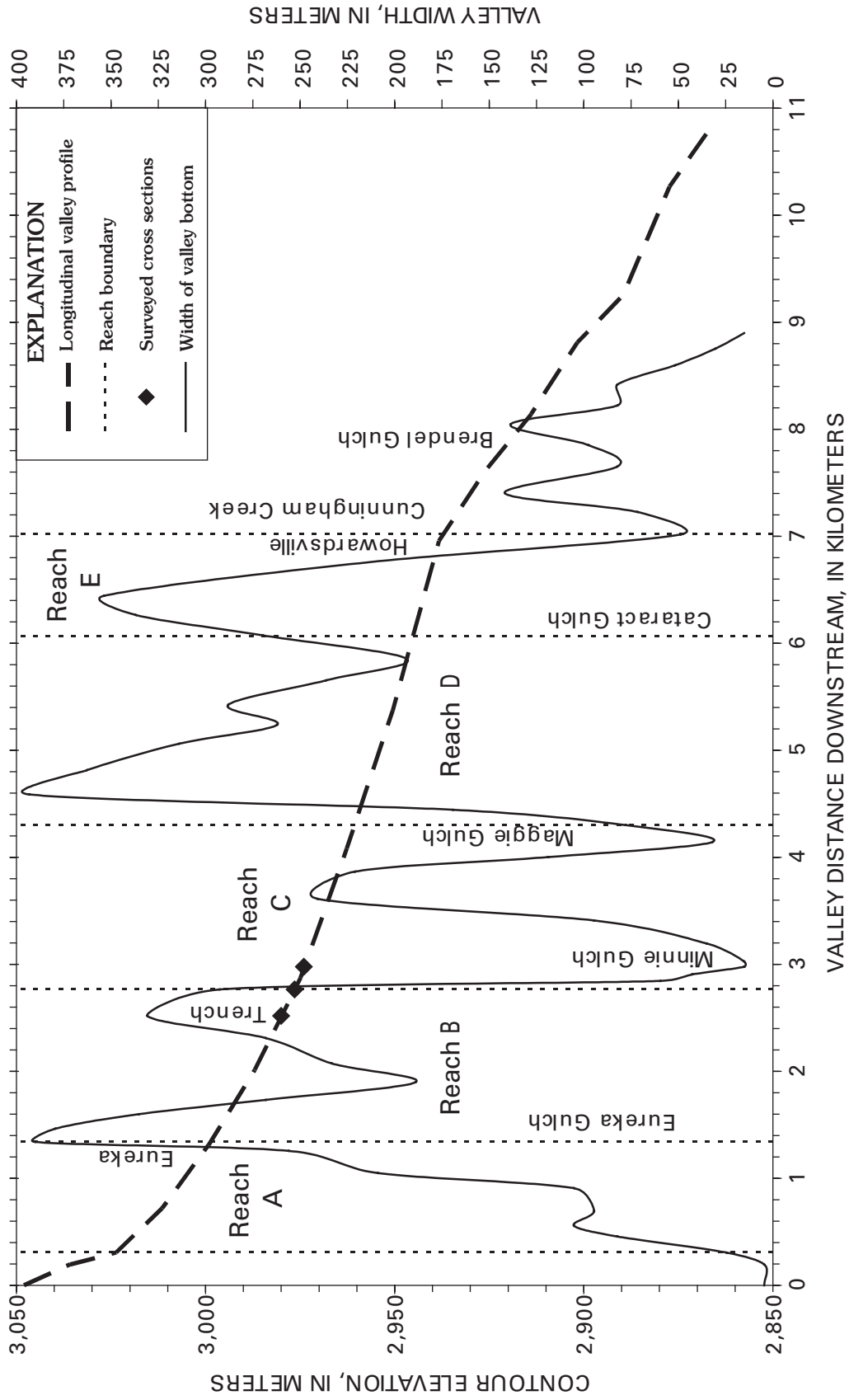
Elsewhere in this chapter we discuss changes that occurred during the first half of the 20th century using flood-plain stratigraphy (pl. 6), and discuss less dramatic changes that occurred during the latter half of the 20th century using the sequence of aerial photographs.

## Spatial Variation in Geometry

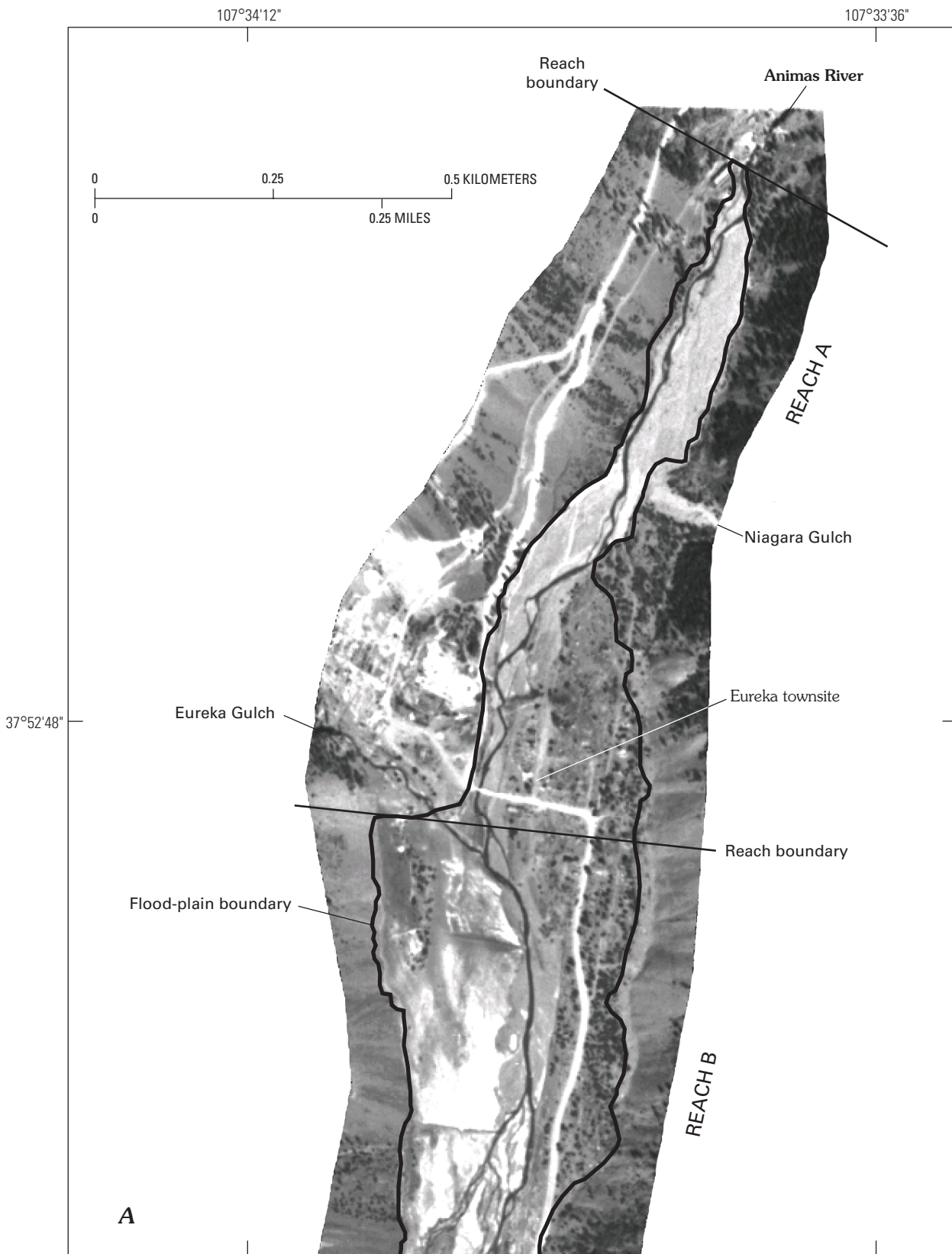
The geometry of the channels and flood plain of our study area is spatially variable (fig. 1) and for that reason is discussed in terms of reaches (fig. 3, table 3, fig. 4), lettered A through E. A major spatial pattern is the variability in the width of the valley floor (figs. 1 and 3). By valley floor we mean the deposits of the Animas River including the active streambeds, the flood plain, and any low terraces present. The repetitive widening and narrowing of the valley floor is the result of constrictions imposed by tributary debris fans and talus cones. The major constrictions are imposed by fans shed from Minnie Gulch, Maggie Gulch, Cataract Gulch, and Cunningham Creek, in conjunction with the fans or cones shed from unnamed watersheds directly opposed to the named watersheds (fig. 1).

A second major pattern is the systematic change in valley gradient. The longitudinal profile of the study reach is fairly smooth and is concave-up (fig. 3), with gradients decreasing down valley from 0.029 m/m in the reach just upstream of the Eureka townsite to 0.008 m/m in the reach at Howardsville. Upstream of the study reach, the river emerges from a steep bedrock canyon, and downstream of Howardsville the river enters another constricted bedrock canyon. Thus, outside of the alluvial study reach the river is bedrock controlled. Inside our study reach the stream has formed itself within its own alluvium (not bedrock controlled), and the stream gradient is not influenced in a major way by the presence of the debris fans. By that we mean there are no inflections in the profile coincident with the debris fan constrictions (fig. 3). In narrower valleys in the region, such as Cement Creek (Vincent and others, this volume), debris fan constrictions have forced the main stream to aggrade upstream of them. This resulted in a segmented longitudinal profile, with the main stream being steep and the streambed being coarse grained on the downstream sides of tributary debris fans. Although the valley gradient was not obviously influenced, the fan constrictions have two consequences. First, the width of any braiding (past or present) was restricted by the narrow space available at the fan constrictions. Second, flow in the wide reaches during major floods must converge as it enters the narrow reaches. This is a partial explanation of the channel patterns as they were in 1998, and in 1951 (fig. 4). The channel was braided with low banks in reaches A and B near Eureka, was confined to a single- or double-thread channel adjacent to the Minnie Gulch and Maggie Gulch debris fans, and was multi-threaded with relatively prominent banks downstream from both fans. The reaches are now discussed individually.

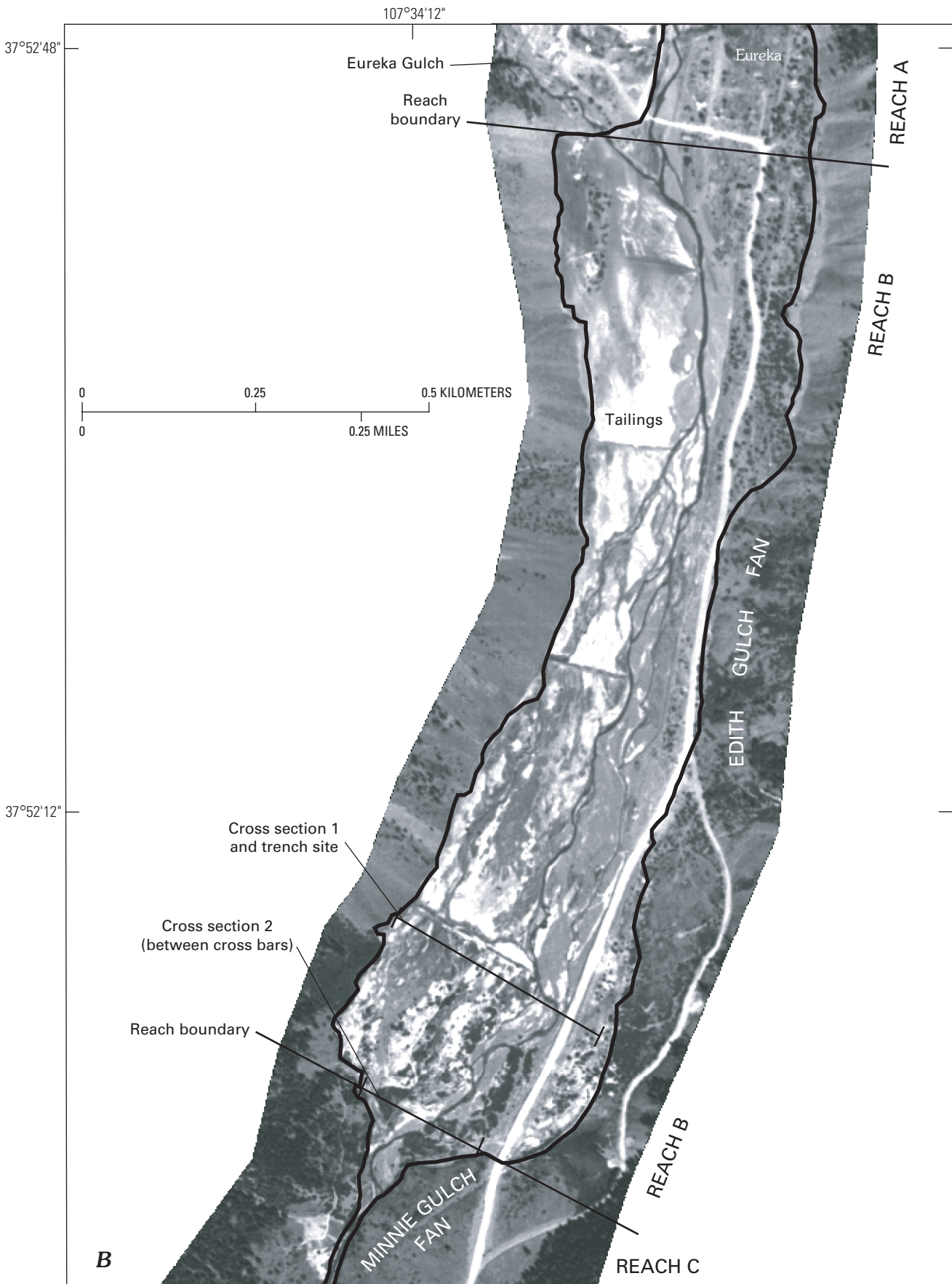
What we refer to as reach A (figs. 3 and 4A) heads at the base of a waterfall in a constricted canyon and extends downstream approximately 0.7 km, past the Eureka townsite, to the Eureka Gulch confluence. The valley floor in reach A is relatively narrow (mean width 170 m) and steep (mean valley slope 0.025 m/m), and the longitudinal profile is strongly concave-up (fig. 3). Elsewhere herein we present evidence



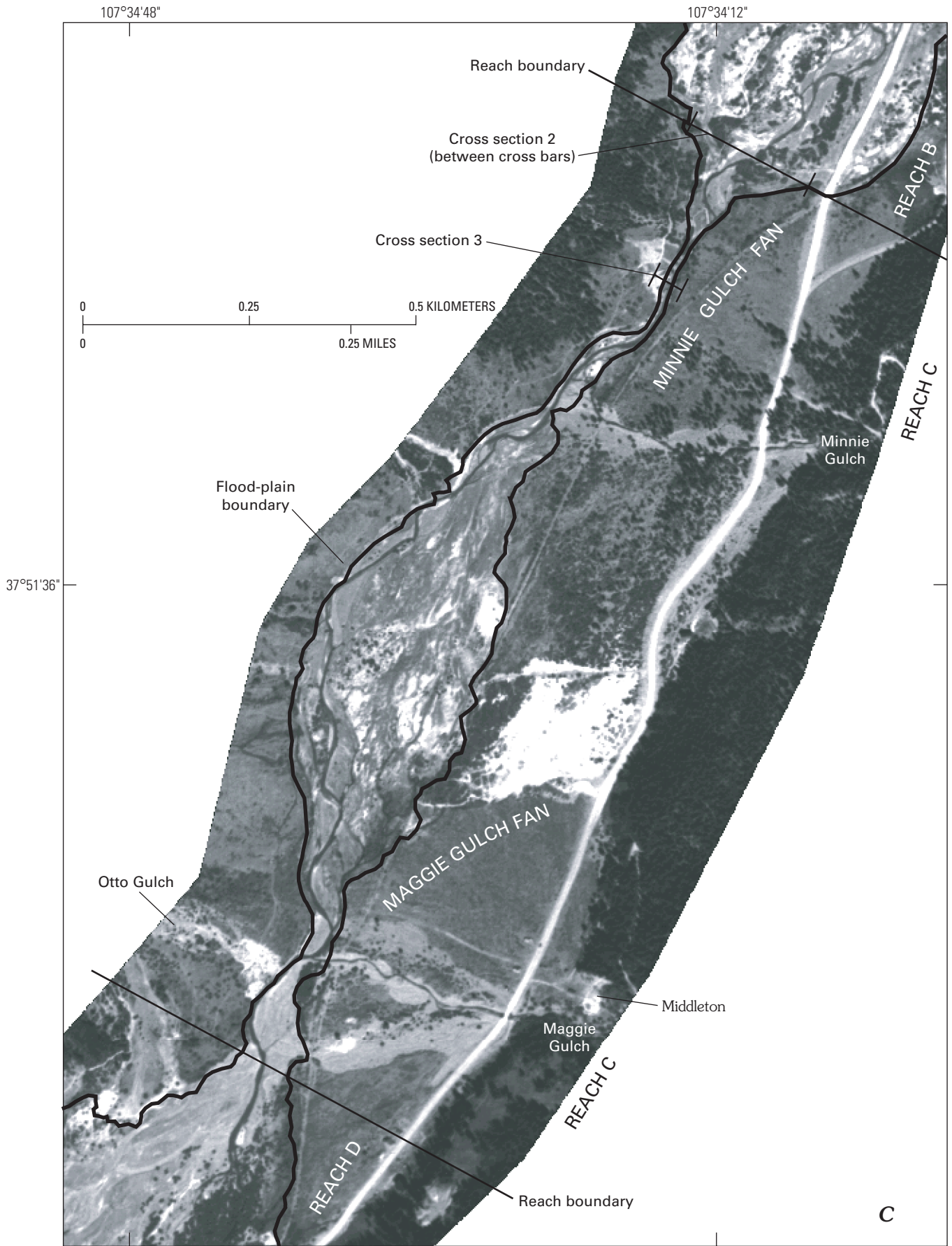
**Figure 3.** Longitudinal profile of upper Animas River study reach, showing the gradient, locations of lettered reaches and the trench (pl. 6), and the spatial variation in width of the valley floor.



**Figure 4 (above and following pages).** Aerial photographs taken in 1951 of upper Animas River valley. *A*, reach A upstream of Eureka; *B*, reach B from Eureka Gulch to north end of Minnie Gulch alluvial fan; *C*, reach C including constrictions caused by Minnie Gulch and Maggie Gulch fans; *D*, reach D from Maggie Gulch alluvial fan to Cataract Gulch alluvial fan, and upper portion of reach E.



**B**



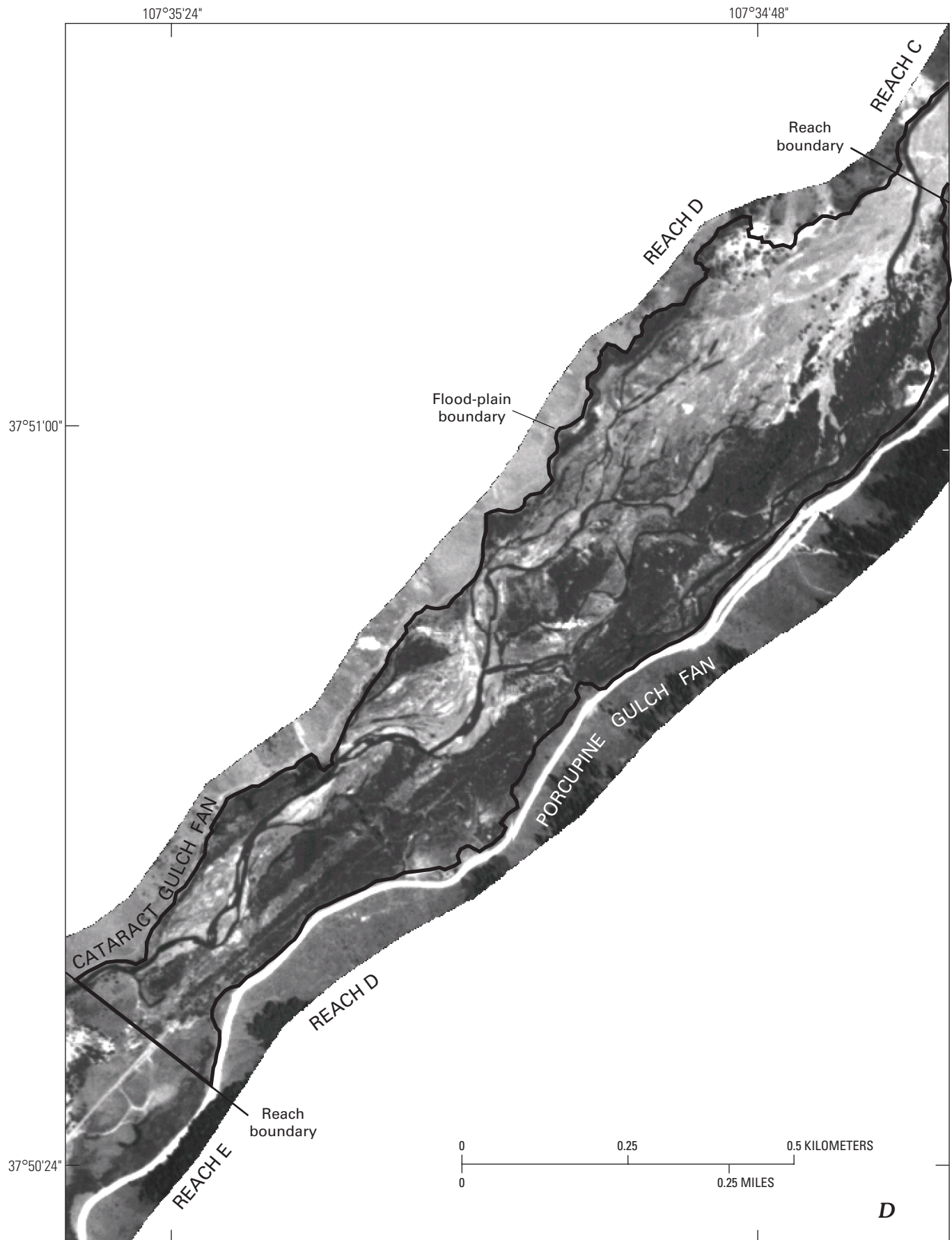


**Table 3.** Dimensions and other physical characteristics of reaches of the upper Animas River.

[Locations of the reaches are indicated in figures 1, 3, and 4. For reach B, 0.2931 km<sup>2</sup> was used for wetland and vegetation calculation, for reasons discussed in the text]

Stream reach letter--	A	B	C	D
Reach length, km	1.000	1.475	1.587	1.730
Valley floor area, km <sup>2</sup>	0.1245	0.4374	0.1751	0.4644
Drainage area, km <sup>2</sup>	67.83	71.25	100.63	108.55
Valley gradient (mean), m/m.	0.025	0.016	0.011	0.009
Valley floor width (mean), km.	0.170	0.290	0.087	0.280

that the Animas River has been, and has the geomorphic tendency to be, fully braided in reach A. The river appears as a single-thread channel on the photograph of figure 4A, however, and that probably is the result of anthropogenic activities. In the field we observed evidence that the streambed had been recently rearranged by heavy equipment upstream of the State Road 110 bridge at the Eureka townsite. That road is visible as a white stripe in figure 4. In order to protect the integrity of the road and bridge (and perhaps the townsite), maintenance crews occasionally rearrange the streambed in order to keep all streamflow passing under the bridge (Rob Robinson, Bureau of Land Management, written commun., 2004). The repetitive nature of that maintenance hints at the sediment transport dynamics of the Animas River in reach A.

Reach B (see photographs of fig. 2) extends from the Eureka Gulch confluence to the north (upstream) end of the extensive Minnie Gulch alluvial fan (fig. 4B). The reach is characterized by a valley floor several hundred meters wide (mean width 290 m) with mean valley slope of 0.016 m/m. The longitudinal profile is concave-up, but the decrease in gradient moving downstream is not as pronounced as it is in reach A. In 1951 (fig. 4B), a large fraction of the valley floor was covered by beds of tailings, visible as irregularly shaped white patches on the photograph. The owners of the Sunnyside mine (AMLI site # 116) physically removed most of those tailings beds before the photograph of figure 2B was taken in 2001. Thus at present, the valley floor consists of an expanse of gravel almost entirely devoid of vegetation (fig. 2B), a portion of which is occupied by the braided channels of the Animas River. The eastern margin of the valley floor is vegetated, and has been protected from the river by the earthen causeway supporting the roadbed of State Road 110. The fact that the roadbed is elevated above the valley floor in reach B suggests that the channels have tended to migrate rapidly or frequently, and (or) that floodwaters have frequently spread out broadly from the shallow channels. Throughout this chapter we demonstrate that the Animas River in reach B experienced major changes during the first half of the 20th century, and less dramatic changes during the second half of the 20th century. The trench (pl. 6) discussed later was located at the downstream end of this reach (fig. 4B).

Reach C extends from the north end of the Minnie Gulch fan to the south end of the Maggie Gulch fan. The valley floor in reach C was severely constricted by two pairs of opposing alluvial fans (figs. 1 and 4C) and the valley-floor width ranged from 15 to 240 m with a mean of 87 m. The valley slope is fairly linear in profile with mean of 0.011 m/m (fig. 3). The river in reach C is a single thread where constricted laterally by the debris fans and multiple-threaded where the valley is wide between the fan-pairs.

Reach D extends from the south end of the Maggie Gulch fan to approximately Cataract Gulch. This reach had a mean valley-floor width comparable with reach B (280 m) and a mean valley slope of 0.009 m/m. The river is multiple-threaded in reach D; however, the channel position has been relatively stable historically. Similar to reach B, the active channels in reach D occupy roughly half of the valley floor. Unlike reach B, the remainder of the valley floor is a low-lying vegetated flood plain locally including wetlands (fig. 4D).

Reach E extended from Cataract Gulch to the Cunningham Creek confluence at Howardsville (fig. 3). No geomorphic measurements were made in this reach because of the presence of an active tailings pond on the valley floor and an earlier mechanical realignment of the main channel.

## Channel Conveyance

In this section discharge calculations are made for channels at three sites in order for us to understand the general magnitude of flow events required to mobilize the streambed and certain tailings deposits. The sites were selected to be representative of the range in modern channel morphology. The trench site (cross section 1) was selected to represent a braided reach, cross section 2 represents sites where the river is multi-threaded, and cross section 3 is a site where the valley floor was constricted by alluvial fans. The site locations are labeled using the cross section numbers in figures 1, 3, 4B, and 4C. Cross sections 1 and 2 were located at the downstream end of reach B. Cross section 3 was located at the upstream end of reach C, where the valley floor is constricted by the Minnie Gulch alluvial fan on the east and by a talus fan shed from an unnamed subbasin on the west (fig. 1).

Field measurements were made during the low-flow conditions of September 1998. We surveyed channel geometry and gradient, using a theodolite with electronic distance meter. Water-surface slope was measured for each cross section over a downstream length of approximately 180 to 195 m, which had vertical fall of from 1.5 to 1.8 meters. The low-flow water-surface slope was relatively consistent through the three surveyed sections: 0.0093 m/m at cross section 1, 0.0090 m/m at cross section 2, and 0.0084 m/m at cross section 3. The mean slope for the 700-m long encompassing reach was 0.0097 m/m. In our calculations we use the local slopes previously mentioned.

Elsewhere in this chapter we present and use slope data derived from topographic contour maps (fig. 3; table 3). For the sake of comparison with the reach with surveyed slope of 0.0097 m/m, the mean slope computed using the three nearest contour lines was 0.0121 m/m.

We determined bed-sediment size characteristics using the “pebble-count” method of Wolman (1954), which involves measurement of sediment-particle intermediate (b-axis) diameters. The results are listed in table 4. Measurements of sediment on the channel banks below the approximate bankfull elevation were made at regularly spaced intervals along the channel at the surveyed cross sections. The measurements excluded tributary-derived debris-flow sediment exposed in cut banks at cross section 3. Sediment in the upper Animas River ranged from pebbles to large cobbles. Minor amounts of coarse sand and small boulders also were found among these sediments, although medium sand and finer grained sediment were almost nonexistent in the streambed surface. The median particle size was 39 mm (medium-sized pebbles) at cross section 2, and 110 mm (small cobbles) at cross section 3 (table 4). The sediment size characteristics at cross section 1 are similar to those at cross section 2.

Cross section 1 coincided with the edge of the trench excavated by this project and is thus depicted as the ground surface on the stratigraphic log (pl. 6). We direct the reader to specific channels using the horizontal distances labeled on the trench log. The portion of the valley floor east of the State Road, east of 287 m, does not receive streamflow from the Animas River and thus is not of concern here. Of the remaining valley floor surface, about 40 percent of the width consists of tailings beds or gravel where the clasts have dark coatings composed of manganese and iron compounds. As these materials are visible in the earliest aerial photographs, we conclude that they were not substantially modified by streamflow during

the latter half of the 20th century. The remainder of the valley floor has been modified by streamflow during recent decades. The active channels consist of one main channel at 155 m, which has one prominent bank 0.9 m high and a point bar, and two wide zones containing numerous shallow channels with indistinct banks and intervening low gravel bars. The two zones of shallow braided channels are located between 107 and 161 m (including the main channel), and between 191 and 286 m. Two discharge calculations were made using the channel cross-sectional geometry shown on plate 6, equation 1, slope of 0.0093 m/m, and  $D_{84}$  of 9 cm. As mentioned in the section on theory, the channel cross sections were subdivided into short increments of relative uniform depth, and the discharge for each increment calculated using equation 1 and the appropriate increment-area; then the incremental discharges were summed to obtain the total discharge.

We estimated the minimum discharge needed to inundate the tailings beds along the trench transect by assigning the water surface to be at the lowest level of those beds, at 7.38 m on the elevation scale of plate 6. This means that we assumed the water surface was horizontal (everywhere at the same elevation) across the width of all zones of flooding. The cumulative top-width of flow was 124 m. The result was a discharge of 42 m<sup>3</sup>/s, which is a rare discharge according to the measurements made at the Howardsville stream gauge (tables 1 and 2). As an annual instantaneous peak at that gauge, this discharge has a recurrence interval of about 10 years (table 2).

That result is used where we discuss the fate of the tailings that remain in our study area. The discharges determined in the remainder of this section are used in the two immediately following sections of this chapter.

We calculated the approximate bankfull discharge at cross section 1 by modeling the flow needed to overtop the gravel bars adjacent to the channels. For this calculation of a moderate flow, it would be inappropriate to assume that the water surface was everywhere at the same elevation. Note that during low-flow conditions the water surface in each channel was at a unique elevation (pl. 6), which is typical of braided streams. For that reason we modeled the flow needed to overtop the gravel bars adjacent to each channel that conveyed low flow at the time the trench was excavated in August of 1988 (pl. 6). The result is four flow-width zones between 106 and 113 m, 147 and 160 m, 195 and 236 m, and 268 and 281 m on plate 6. The cumulative top-width of flow was 69 m, and the result was a discharge of 17 m<sup>3</sup>/s.

Cross section 2 is located 217 m downstream from cross section 1, and along that distance channels begin to converge as they enter the valley floor constriction caused by the two fans (figs. 1 and 4B). At cross section 2, both the channels and flood plain are distinctly different from those upstream in reach B. The channels have transitioned from being braided (multiple shallow channels with largely indistinct banks) to what we call multi-threaded: more than one channel but most having steep and relatively high banks. At cross section 2, the valley floor is about 240 m wide, and about 60 percent of that width consists of flood plain vegetated by willows and

**Table 4.** Streambed sediment characteristics of the upper Animas River near Eureka.

[The critical shear stress for initiation of motion of the median sediment size was calculated with equation 4 and the given Shields parameter ( $\tau_c$ )]

		Location	
Cross section (fig. 1)		2	3
Downstream distance	km	2.77	2.98
Stream reach		B	C
Sediment size characteristics			
1st percentile size	mm	6	13
16th percentile size	mm	21	53
Median sediment size	mm	39	110
84th percentile size	mm	91	196
99th percentile size	mm	145	311
Mean size	mm	51	125
Standard deviation	mm	37	73
Geometric mean	mm	44	101
Standard deviation		2.1	1.9
Critical shear stress			
Using $(\tau_c)_c = 0.030$	N/m <sup>2</sup>	19.5	55

grasses. During low-flow conditions four channels conveyed water. One channel was small, and a second was a beaver pond at the time of the field measurements. The other two channels had steep banks about 0.6 m high. One channel was about 16.5 m wide and contained a mid-channel bar, and the other channel was 12.5 m wide and did not contain a bar.

We calculated the approximate bankfull discharge at cross section 2 by modeling the flow needed to overtop the banks of the two main channels. The consequence of ignoring the small channel and the beaver pond cannot be evaluated with available data, but the result is likely an underestimate. The discharge calculations were made using the surveyed cross-sectional geometry, a slope of 0.009 m/m,  $D_{84}$  of 9 cm, and equation 1. The cumulative top-width of flow was 27 m, and the result was a discharge of almost 16.6 m<sup>3</sup>/s—essentially the same as the 17 m<sup>3</sup>/s bankfull discharge calculated for cross section 1.

Cross section 3 was located 255 m downstream from cross section 2, and along that distance the fan constrictions cause all channels to converge into one (figs. 1 and 4C). No flood plain was present at cross section 3, and the channel is shaped like a parabola with high banks exposing fan sediment. As there was no clear evidence of bankfull stage at cross section 3, we solved the flow equation for the stage required for the channel to pass a discharge of 17 m<sup>3</sup>/s. We used the surveyed cross-sectional geometry, slope of 0.0084 m/m,  $D_{84}$  of 20 cm, and equation 1. The result is that a flow top-width of 11 m, maximum depth of 1.14 m, and mean depth of 0.75 m will convey 17 m<sup>3</sup>/s.

As flow moves from cross sections 1 to 2 to 3, the channel geometry and hydraulics change. The channels transition from being braided (multiple shallow channels with largely indistinct banks), to what we call multi-threaded (more than one channel but most having steep and relatively high banks), to a fully confined single channel. For the modeled discharge of 17 m<sup>3</sup>/s, the calculations indicate the following changes moving downstream. Flow width diminishes by about 85 percent, decreasing from 69 to 27 to 11 m. Mean flow depth increases by more than a factor of 3, increasing from 0.22 to 0.41 to 0.75 m. Mean flow velocity nearly doubles, increasing from 1.1 to 1.5 to almost 2 m/s.

## Bed Sediment Mobility

We next evaluated the mobility of the bed sediment at the three cross sections, using equation 4 and the assumptions contained in the section on theory. Using the results for the modeled discharge of 17 m<sup>3</sup>/s, and the measured sediment characteristics (table 4), we calculated whether the local shear stress on the bed exceeded the critical shear stress for initiation of motion. By local shear stress we mean that within each width increment of the cross sections.

For a discharge of 17 m<sup>3</sup>/s at cross section 1, initial motion of the bed would occur over cumulative width of 26 m or about 22 percent of the total width of the bed. For that discharge at

cross section 2, initial motion of the bed would occur over cumulative width of 25 m or slightly more than 90 percent of the total width of the bed. For that discharge at cross section 3, initial motion of the bed would occur over cumulative width of almost 7 m or about 62 percent of the total width of the bed.

The volumetric rate of bed load transport was calculated at the three cross sections using equation 6 and the assumptions contained in the section on theory. A model discharge of 17 m<sup>3</sup>/s was used. The resulting bed load transport for cross section 1 was 22 m<sup>3</sup>/hr, and for cross section 2 it was 15 m<sup>3</sup>/hr. The bed load transport calculations involve a variety of assumptions, and the results are highly sensitive to slope. In the calculation for cross section 2, for example, if a slope of 0.0095 m/m had been used (instead of 0.0090 m/m) the resulting transport rate would have been 22 m<sup>3</sup>/hr. Thus, given the uncertainties in the calculations, we consider the bed load transport rates at the upper two cross sections to be indistinguishable.

From the calculations for cross section 3, using the properties of the cobble gravel observed there during low-flow conditions, we learned that the Shields stress on the bed (equation 5) did not exceed 0.05. Thus the cobble gravel would not experience significant motion, rather some slow rate of marginal transport. Calculation of the marginal sediment transport at this location is not necessary to achieve the goals of this project. From the calculations for the upstream cross sections, it seems clear that considerable pebble gravel would be delivered to cross section 3 during bankfull flows. Assuming the entire bed was covered by pebble gravel, the calculated transport rate was 78 m<sup>3</sup>/hr, but that is far in excess of the calculated supply of pebble gravel from upstream. We repeated the calculation assuming 20 m<sup>3</sup>/hr of pebble gravel was transported in the thalweg (the lowest portion of the channel bed) of cross section 3, and learned the width of the zone of pebble gravel transport would be on the order of 1 m, or about 9 percent of the bed width. We suspect that the cobble gravel is something of a lag deposit, moving during major floods but only occasionally (slowly) during normal high flows. During normal high flows, however, the calculations show that all pebble gravel supplied from upstream would be transported through the confined reach.

It is possible to conclude the following, considering the limitations of the analysis. The bed material of the study area can be mobilized by bankfull flows, and pebble gravel is particularly mobile. As we discuss in the next section, bankfull flow may have a recurrence interval on the order of 2 years; thus the bed material is mobilized frequently. At the downstream end of reach B, the Animas River transitions from being fully braided, to multi-threaded, to a single confined channel. Through that transition the changes in flow width, depth, and velocity are substantial. Yet, it appears that during bankfull flows the bed load sediment transport rate may be uniform (not changing in the downstream direction) and thus neither substantial net-aggradation nor net-erosion of the bed is expected. That reach at least, may be in geomorphic

equilibrium, no net-changes in bed level during channel forming flows, even though the channel geometries change moving downstream in substantial ways.

The reach encompassing the three cross sections has a relatively uniform slope, in comparison to the profile of our 7-km long study area as a whole (fig. 3). We develop the sediment transport implications of the convex longitudinal profile in the next section.

## Implications of Channel Patterns

One objective of this study was to identify the range of channel characteristics likely to be in equilibrium with the existing streamflow regime, valley morphology, and the caliber and supply rate of sediment in the upper Animas River valley. We asked whether the stream channels could have been meandering in the past or could be in the future. We evaluated this in two ways, first by comparing data for the Animas River to empirical relations for other rivers.

All other factors being equal, valleys tend to have braided channels as the gradient increases beyond some threshold condition. Leopold and Wolman (1957) demonstrated that channel gradient and bankfull discharge could be used to define a threshold condition between channels with a meandering versus braided pattern. Leopold and Wolman (1957) used a broad definition of braiding, including both fully braided streams such as those in our area located above the trench site and multi-threaded channels such as those located downstream of the trench site (figs. 2 and 4). They also avoided sites where channels were laterally confined, such as at our cross section 3. The Leopold and Wolman (1957) threshold is illustrated in figure 5, where sites plotting above the line had braided channel patterns whereas those plotting below the threshold had meandering patterns. Subsequent work has shown that the tendency to braid is influenced by sediment supply rate (Schumm and Khan, 1972) and that the threshold is influenced by the grain size of bed and bank sediment (Osterkamp, 1978; Begin, 1981). Streams with high sediment supply tend to be braided, and sand-bedded streams braid at lower gradients than do gravel-bedded streams. There are other nuances involved with the threshold of braiding; nonetheless, the Leopold and Wolman (1957) relation remains a rough statistical discriminator between meandering and braided patterns where the bed sediment is relatively fine grained gravel (Carson, 1984), such as the bed of the Animas River in our study reach.

In order to place data for the Animas River in figure 5, we had to estimate the magnitude of bankfull flow moving down the study reach. Hydrologists have long recognized that flood discharge (in perennial streams) increases moving down-valley as tributaries enter and thus increase drainage area. This phenomenon must be considered here because numerous tributaries join the Animas River within the 7-km long study reach

(fig. 1). Leopold and Miller (1956) studied streams draining mountains near Santa Fe, N. Mex., and related bankfull discharge ( $Q_{Bf}$ ) to drainage area ( $A_d$ ) using a power function

$$Q_{Bf} = a(A_d)^b \quad (7)$$

Conceptually, if precipitation were uniform throughout a watershed having uniform infiltration properties, runoff would be directly proportional to watershed area. In other words the exponent of equation 7 would be  $b = 1$ . This is generally not the case for flood events, however, because runoff is not generated from all portions of large watersheds (whereas it might be for small watersheds). For example, the exponent typically ranges from  $b = 0.7$  to  $b = 0.9$  (Dunne and Leopold, 1978). In the Leopold and Miller (1956) study, the exponent was  $b = 0.8$ ,  $Q_{Bf}$  had a recurrence interval of 2.3 years, and the coefficient was  $a = 0.52$  for metric units of discharge ( $m^3/s$ ) and drainage area ( $km^2$ ). An alternative scaling relation was developed from measurements of low flow. Kimball and others (this volume, Chapter E9) made synoptic discharge measurements at numerous locations in the upper Animas River study area on August 14, 1998. The low-flow discharges ranged from  $0.357 m^3/s$  above Eureka Gulch to  $3.56 m^3/s$  at the Howardsville gauge (fig. 1). Casting these data in the form of equation 7 results in an exponent of  $b = 1.8$ .

We started by assuming that bankfull discharge for the study area has a recurrence interval of 2 years, and ultimately tested that assumption. As shown in table 2, the flow with a 2-year recurrence interval ( $Q_2$ ) at the Howardsville gauge has a magnitude of  $27.7 m^3/s$ . The sites where low flow was measured were plotted on maps, and the drainage area upstream of each site was determined from the topographic maps. We estimated  $Q_2$  at each site by scaling (decreasing)  $27.7 m^3/s$  using equation 7 and exponents of  $b = 0.8$  and  $b = 1.8$ . The results are plotted in figure 5, with the sites labeled using the letter of the reach in which they were located. The two methods yielded nearly identical estimates for  $Q_2$  above Cunningham Creek, the first tributary upstream of the gauge, but they vary by a factor of about three in reach A above the Eureka townsite (fig. 5). Because the exponent 1.8 is greater than 1, use of that exponent likely results in unrealistically low estimates of  $Q_2$  for sites upstream of the gauge.

We tested our assumptions by using the calculated bankfull discharge near the trench site (fig. 1). As discussed in the section titled, "Channel Conveyance," a bankfull discharge of  $17 m^3/s$  was estimated by calculating the flow needed to overtop the active bars at the trench site and at cross section 2. The combined assumptions that bankfull discharge was equivalent to  $Q_2$ , and that an exponent of 0.8 in equation 7 was appropriate for the study area, result in a discharge of  $15 m^3/s$  that closely approximates the bankfull discharge determined using field measurements. Use of the exponent of 1.8 results in a discharge of  $7.5 m^3/s$ , a low value, as expected; but the important issue at hand is that we not grossly overestimate bankfull discharge and erroneously place the results into the braided field of figure 5.

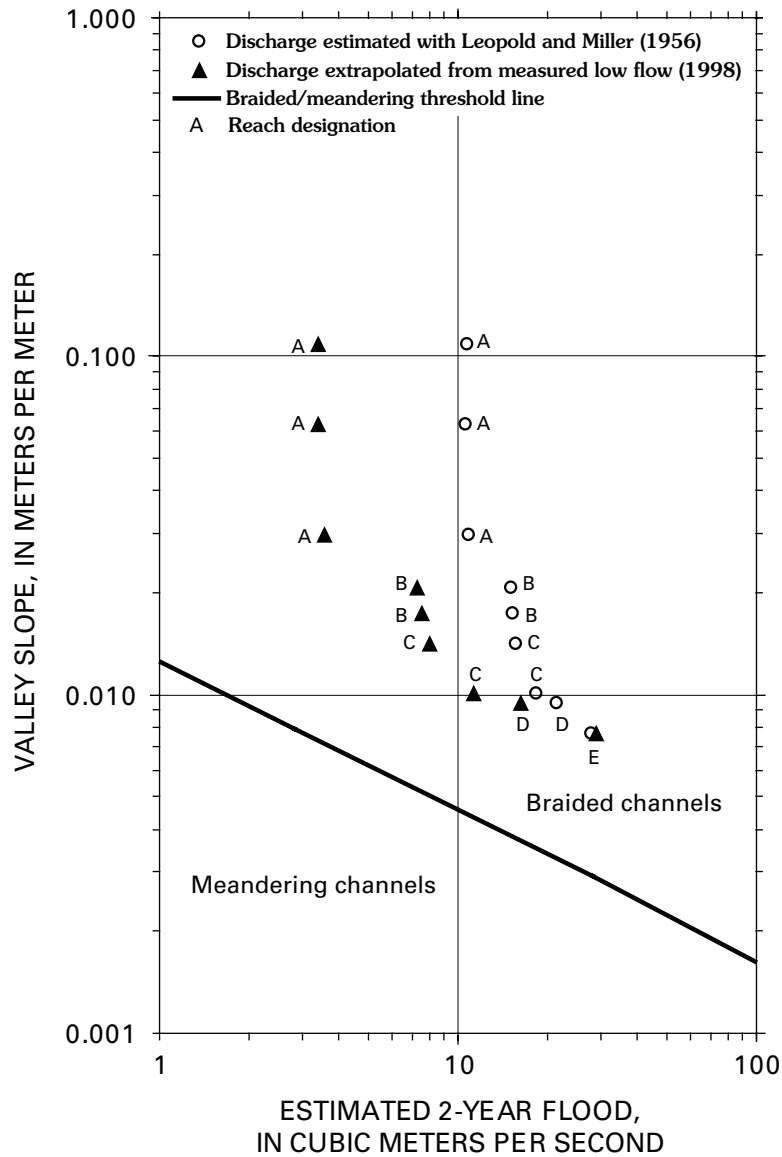


**Figure 5.** Threshold relation between valley slope and bankfull discharge for braided and meandering streams, modified from Leopold and Wolman (1957). The 2-year discharge for the Animas River was used as a proxy of bankfull discharge.

Data for all study reaches plot above the threshold line in figure 5, within the field for braided streams. Data for reaches A and B plot the highest on the diagram. In conclusion, the Animas River in the study area was likely never a classical, single-thread meandering stream, and this is certainly true for the reaches near Eureka. This simple comparison with data for other streams suggests that the Animas River has the propensity to be multi-threaded, or fully braided where not confined by alluvial fans or dense brush on the flood plain. We next addressed the channel pattern issue by exploring the sediment transport dynamics.

Meandering streams persist in the landscape because sediment transport is uniform along the length of the stream, over time scales of individual floods. Stream braiding is

caused by localized sediment deposition resulting in shoaling and branching of the flow. Thus, in order for a single-thread channel to persist, local, even temporary bed aggradation cannot be large relative to the channel depth during a flood. Otherwise the channel may widen, adding sediment and promoting shoaling, or excess flow will pass overbank likely creating additional channels. Spatially uniform sediment transport is accommodated by adjustments in channel geometry, in response to changes in independent variables. For example, at the downstream end of reach B, the narrowing valley floor forces channels to converge, and the character of the channels to change dramatically, yet our calculations indicated that sediment transport may be uniform during bankfull flows. A major independent variable (over time scales of individual floods)

for the Animas River is the 72 percent decrease in valley slope from 0.029 to 0.008 m/m within our study area (fig. 3). From a sediment transport perspective that decreasing slope is counterbalanced, at least in part, by the discharge increasing downstream. Here we pose a thought question: in our study area is it possible for bed load transport to be uniform within a single-thread channel?

Consider a hypothetical single-thread channel running the length of our study area, which has imposed upon it the existing valley gradient, general bed material, and flow regime. By flow regime we mean how discharge increases downstream. We utilized the discharge with 2-year recurrence interval (27.7 m<sup>3</sup>/s at the stream gauge) scaled as a function of drainage area raised to the 0.8 power, calculated previously. That discharge pattern is presented, and the valley profile is reproduced, in figure 6. For simplicity, the hypothetical channel is rectangular in cross section and its width increases downstream as a function of discharge raised to the 0.5 power. It has long been recognized for meandering streams that bankfull width scales as a function of bankfull discharge, and a typical exponent is 0.5 (Dunne and Leopold, 1978, p. 639). We arbitrarily assigned the width to be 8 m at the head of reach A, and used that scaling relation to obtain the widths downstream. The width was 11.3 m at the downstream end of reach D. We ignored any supply of sediment from tributaries, and as it turns out that assumption was not detrimental to this calculation. We assumed the streambed to be uniformly composed of pebble gravel with  $D_{50}$  of 4 cm and  $D_{84}$  of 9 cm. Calculations were made for subreaches, each bounded by the contour lines from

which slope was calculated. As such there are two subreaches for both reach A and reach B, shown by the breaks in slope in figure 6.

Flow depths were calculated using equation 1, and the discharge and width specified for each subreach using the approach discussed in the preceding paragraph. The depth nearly doubled, increasing from 0.41 m near the head of reach A to 0.74 m at the downstream end of reach D. The boundary shear stresses for the hypothetical flow, calculated using equation 3, decreased by more than half through the study area. The calculated shear stress values for each subreach are shown in figure 6, along with a smoothed profile emphasizing that most of the decrease occurred within reaches A and B. Uniform sediment transport in our hypothetical channel requires uniform boundary shear stress, and this was not achieved. If sediment were in transport at the upper end of reach A, then sediment must deposit as boundary shear stress decreases downstream. The necessity for sediment deposition would be exacerbated if tributary streams also delivered sediment to the trunk stream.

In order to demonstrate the general magnitude of sediment deposition, we calculated hypothetical bed load sediment transport rates using equation 6. Sediment transport rates decreased by 86 percent, from 316 m<sup>3</sup>/hr near the head of reach A to 43 m<sup>3</sup>/hr at the downstream end of reach D. Most of that decrease occurred within reaches A and B, and we considered changes in sediment transport in reaches C and D to be essentially not detectable. An estimate of deposition rate was made by subtracting the transport rate in a subreach from that

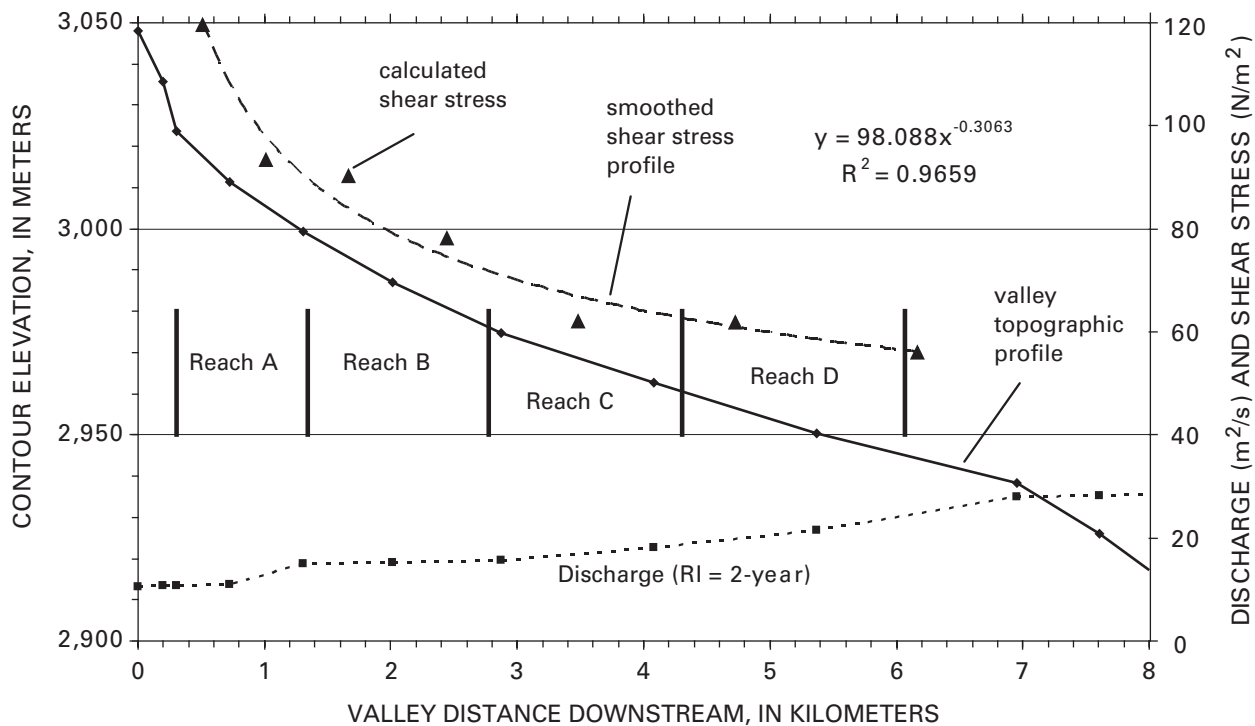


**Figure 6.** Pattern of boundary shear stress for a hypothetical single-thread channel conveying a flow with 2-year recurrence interval (RI).

in the subreach just upstream. Technically the results are for the solid-volume of particles, so a porosity of 30 percent was used to convert particle-volume to bulk-volume of the deposit. The deposit was assumed to spread out uniformly over the width and length of a subreach. The results were a deposition rate of about 4 cm/hr in the lower half of reach A, and less than 1 cm/hr in the lower half of reach B. If the hypothetical flow were sustained, the channel in the lower half of reach A would be full of gravel in about 10 hours, and the channel in the lower half of reach B would be full in about 2 days. Recall that as a daily mean discharge, the flow with 2-year recurrence interval was equaled or exceeded at the stream gauge approximately 0.14 percent of the time on average (table 2), or 12 hours per year. When channels fill with gravel, flow is forced around the deposit, and a braiding pattern is the inevitable result.

The results of the calculation for this hypothetical channel allowed us to conclude the following. A meandering stream (self-sustaining, single-thread, gradually widening channel) cannot persist in reaches A and B. Aggradation is inevitable, because of the influence the rapidly decreasing valley slope has on sediment transport. Perhaps an engineered channel resembling a meandering stream could be designed to accomplish uniform sediment transport. The width of such a stream would need to gradually narrow, and the banks would have to be hardened, and very high, to prevent the river from widening or escaping onto the previous braid plain. Natural processes would not create such a channel. Natural processes did create a channel network with spatially varying geometry that did accommodate uniform bed load transport. In subsequent sections we use a variety of evidence to demonstrate the following. In prehistorical times reach A was broad, shallow and braided. Through reach B the Animas River transitioned

into being multi-threaded; each thread was relatively narrow, with meter-high banks composed of cohesive flood-plain silt strengthened and protected by a dense thicket of willows. That bed load transport was uniform is evidenced by the fact that during the thousand years before A.D. 1900 the channels did not aggrade appreciably, as will be demonstrated.

## Sources of Sediment Supplied to the River

In order to understand the origin and ages of metal-laden sediment in our study reach, and to help identify the causes of channel change, we evaluated the various sources and rates of supply of sediment to the river. This involves an understanding of the history of mining and other land-use practices, in particular the milling of ore (fig. 7). In this section we present various measurements as they were reported, in feet, miles, and tons. Presumably “tons” means U.S. short tons (2,000 pounds).

### History of Ore Milling

Jones (this volume) has discussed the history of mining in the whole region. The history presented herein focuses on the mills in the headwaters area of the upper Animas River that produced significant tailings, which might have impacted the river between Eureka and Howardsville. We adopt the names and site numbers (given in parentheses) of Church, Mast, and others (this volume, Chapter E5, fig. 5). The Sunnyside-Thompson Mill (site # 113) was located in upper Eureka

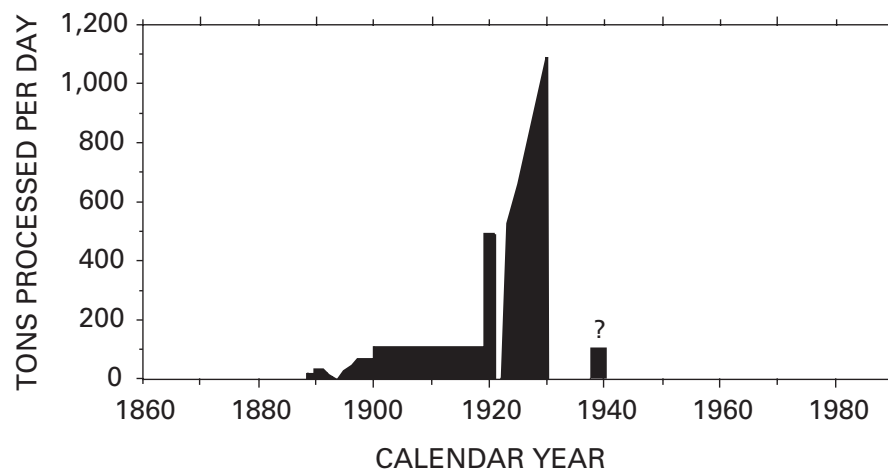


**Figure 7.** Combined ore processing rates for the succession of mills in the town of Eureka and in Eureka Gulch. These rates (from Bird, 1986; Marshall, 1996; and Sloan and Skowronski, 1975) were quoted in “tons,” which presumably means U.S. short tons. (To convert short tons to metric tons, multiply by 0.907; ?, production rate uncertain.)

Gulch about 5.5 km from the Eureka townsite and close to the Sunnyside mine on the shores of Lake Emma. The Sunnyside Mill # 1 (site # 158), sometimes called the Midway Mill, was located about 3 km up Eureka Gulch from its confluence with the Animas River. The Sunnyside Mill # 2 (site # 165) and the Sunnyside Eureka Mill (site # 164) were both located in Eureka. There were also various mines and mills (sites # 24, # 26, and # 27) near the Animas Forks townsite, which is on the Animas River about 7 km upstream of Eureka.

The first prospectors explored the area in 1860; however, the Civil War brought those expeditions to a halt (Bird, 1986). In 1871 expeditions resumed and the prospectors learned that placer mining would not be viable, but that money could be made mining hard rock. Mining did not begin in earnest until after the September 13, 1873, Brunot Treaty, which ceded land from the Ute Indian tribe. Through the 1870s mining produced valuable metals, but the quantity of ore (hand sorted and “high-graded” by miners and shipped from the area on mules and burros for processing) was relatively small. Mines around Animas Forks, for example, “were worked in the 1870’s and produced 800 tons of ore” (Marshall, 1996, p. 140). Compared to later production, 800 tons in a decade is paltry and none of that ore was milled on site. The Sunnyside mine ultimately became famous as the biggest gold mine in Colorado history, but in 1879 its “workings consisted of one shaft 10 feet deep and one drift 30 feet in length” (Bird, 1986, p. 16).

During the 1880s and 1890s mining (and eventually milling) occurred at a limited scale, and was intermittently disrupted by mechanical failures, natural disasters, and economic setbacks. In 1888 the first mill (a “ten-stamp” mill) was constructed close to the Sunnyside mine and located “just below Lake Emma” (Bird, 1986, p. 29), meaning that the sand-sized tailings were discharged into the Eureka Gulch drainage. Late in 1889 the Sunnyside Mill # 1 began operation next to the creek in Eureka Gulch and processed 15 tons of ore per day. This early mill would have been much like that shown in figure 11 of Jones (this volume). Stamps were added to that mill in 1897, increasing capacity to 50 tons per day. After the Silverton Northern Railroad tracks reached Eureka in 1896 (Sloan and Skowronski, 1975), the first mill in Eureka (Sunnyside Mill # 2) was constructed in 1899 and began production in 1900 (Marshall, 1996). It was designed for a capacity of 125 tons per day; in figure 2 it is visible as a dark rectangle on the right side of the mouth of Eureka Gulch. It was similar to that shown in figure 12 of Jones (this volume).

These stamp mills were inefficient. A “stamp” was a piston device used to crush ore to the size of sand, and economical minerals were then concentrated using various means, generally mechanical, for railroad shipment to smelters. The remaining sandy material was discharged from a mill’s tail-race into the Animas River or its tributaries, and these tailings contained metals. In 1899 “60 percent of the values ended up in the tailings that were carelessly dumped into Eureka Creek” (Bird, 1986, p. 34). These “values” were unrecovered gold and

silver, but the tailings also included pyrite, galena, pyroxmangite, and some sphalerite hosting other metals such as lead and zinc. Around 1900, the Sunnyside Mill # 2 recovered less than 50 percent of the metals contained in lead-zinc ores being exploited at that time, having been designed to recover gold (Bird, 1986, p. 68). The stamp mills were thus inefficient at recovering minerals of economic value at the time, and the tailings released then contained elements such as lead and zinc that are of concern now.

The stamp mills were generally in full production from 1900 to 1918. Late in 1904 the Silverton Northern Railroad began service to the town of Animas Forks and the new Gold Prince Mill (site # 27) located there. The Gold Prince Mill had a reported capacity of 500 tons per day (Marshall, 1996), but production from the mill (and others in the area) was probably small. It was dismantled in 1910, and railroad service to Animas Forks was abandoned in 1916 (Sloan and Skowronski, 1975). Uniquely, the Sunnyside mine remained profitable, because its ores were rich in gold. In 1910 it consisted of “ten miles of underground workings” and the Sunnyside Mill # 2 was processing 3,500 tons of ore per month (Bird, 1986, p. 114). In 1912 an electrostatic zinc recovery plant was added to the Sunnyside Mill # 2 (presumably reducing zinc concentrations in the sand-sized mill tailings), and that and rising zinc prices probably saved that mine (unlike the others) during World War I.

The year 1918 marked the beginning of a new era. The new Sunnyside Eureka Mill was completed; it is shown in figure 19 of Jones (this volume). This mill was capable of processing as much as 600 tons of ore per day using a revolutionary selective flotation process that increased mill efficiency and profitability (Bird, 1986). Ore crushing techniques were also significantly improved at this time, resulting in fine-grained tailings composed of silt-sized and finer (<300 mesh) particles. The old stamp mills were abandoned. Full-scale production was hampered, however, because of various disasters, until the end of 1919; but then the Sunnyside mine was forced to close late in 1920 because metal prices plunged. In the fall of 1921 the mine reopened and the boom years began. By 1923 the mine was producing 16,000 tons of ore per month, 20,000 tons per month by 1925, and broke all records by producing 1,100 tons of ore per day by 1929 (Bird, 1986). After the October 1929 stock market crash, however, the Sunnyside mine struggled and then closed in September 1930. The mine was reopened again in 1937, faltered, and closed again in August 1939. At the time of closing, a total of 2,500,000 tons of ore had been mined and milled, producing \$50,000,000 in metals—and Eureka became a ghost town (Bird, 1986).

Figure 7 illustrates the trend in the quantities of ore milled by the Sunnyside mine. About 80–90 percent of the processed ore was released as tailings (King and Allsman, 1950). Using the 80 percent value and the ore processing rates in figure 7, mill tailings production rates were calculated and converted to metric tons. Most coarse-grained stamp mill

tailings were produced between 1900 and 1918, at rates in excess of 35,000 t (metric tons) per year. Most fine-grained tailings were produced after 1921 and before 1930, at rates between 150,000 and 330,000 t per year.

### Other Sources of Sediment

The rates of sediment supply from other sources are estimated for comparison with that from milling. The calculations herein include the watershed area of Eureka Gulch, so we are discussing the delivery rate to the top of reach B. Known rates of hillslope sediment yield span 6 orders of magnitude, from 0.004 to 500 t/hectare/year. These two numbers are for undisturbed primeval forests and for intensely disturbed croplands and construction sites, respectively (Dunne and Leopold, 1978). The prehistorical sediment production rates for the upper Animas River setting were probably at the low end of that spectrum, around 0.01 or perhaps 0.1 t/hectare/year, resulting in total yield from the 73.6 km<sup>2</sup> watershed of perhaps 74 or 740 t per year.

Logging probably did not increase sediment yields significantly, because only 12 percent of the watershed is forested and only a fraction of the original forest was logged. The area was grazed, and grazing can increase sediment yields by perhaps 10 times (Dunne and Leopold, 1978), but only about half of the headwaters area of the upper Animas River basin is soil mantled and thus susceptible to increased erosion by grazing, which by nature of the high altitude is seasonal. Grazing (and to a lesser extent logging) may have increased the watershed sediment yield by hundreds to a few thousand metric tons per year.

Erosion of mine-waste dumps also supplied sediment to streams. In the Animas River basin upstream of the trench site, there are 24 mine shafts, 209 mine portals, and 679 prospect pits, based on the mining symbols on the USGS topographic maps. Each of these excavations has a pile of waste rock, and each waste dump contains about 200 t of material covering an area of about 50 m<sup>2</sup>, on average (J.T. Nash, oral commun., 1999). Together the waste dumps cover an area of approximately 4.5 hectares. An erosion rate of 100 t/hectare/year is typical for disturbed land in general (Dunne and Leopold, 1978). If this is appropriate for mine dumps, collectively the dumps in the basin lost 450 metric tons of sediment per year, but only a fraction of the coarse sediment mobilized from dumps reached streams because most mine sites are located high on hillslopes several kilometers from streams.

In conclusion, prehistorical sediment production rates for the watershed upstream of reach B may have been on the order of 74–740 t per year. Human activities, such as logging and mining (but excluding ore milling), may have increased sediment production to a few thousand metric tons per year, or less. Ore milling in the early part of the 20th century, in contrast, resulted in tailings being supplied directly to the fluvial system at rates varying from 35,000 to 330,000 t per year.

## Photographic Evidence of Change and Recovery

Matched pairs of photographs taken over various intervals of time have been used as a scientific tool for a century or more (Rogers and others, 1984), and have been particularly useful for documenting changes in the physical landscape (Malde, 1973) and changes in vegetation communities (Hastings and Turner, 1965). Oblique photographs allow qualitative evaluation, at least, of changes occurring during periods as long as 150 years. Aerial photographs allow quantitative evaluation, using modern computational techniques, of changes over periods generally less than 60 years. We have used both types of photographs to help understand historical changes that have taken place in the study reach.

### Early Oblique Photographs

We inspected historical photographs in order to understand the character of the Animas River during the early days of mining, before milling and other human activities became intense. For that reason attention was paid toward authentication of photograph dates.

The earliest picture of the study reach that we were able to find is a print based on a photograph taken in 1877 (fig. 8) and shows reach A and the town of Eureka (fig. 4A), which was established in 1876. The title on the print gives the 1877 date and states that it was “photographed by P.A. Felt.” The picture was clearly reproduced using a printing press, and therefore the accuracy of the image depends in part on the method used to transfer the photograph to the printer’s plates (Ostroff, 1981). Certain lithographic plates were made directly from negatives, similar to the way photographic prints are made, and the result was a highly accurate image (although an artist could make changes like adding clouds). Other plates were wood engravings made by either tracing directly or copying by eye from a photograph, and the results were variable in accuracy (Ostroff, 1981). Based on the high contrast and absence of gray-tone range, we believe the image in figure 8 was printed from a wood engraving. We compared the cliffs and strips of trees in center-left background to photographs (see fig. 2) and found they were rendered accurately. For that reason, we believe figure 8 accurately depicts the Animas River as it was in 1877. Felt took the photograph 1 year after Eureka was established and 6 years after miners arrived in the area. Before 1877 it is likely the miners had only two impacts of potential significance to this discussion. One was the cutting of trees for firewood and building material, and indeed what appear to be tree stumps are visible in center foreground of figure 8. No tree stumps are visible adjacent to the channel, however, so apparently the Animas River in reach A was not previously lined with riparian trees. The second impact was the use of beaver as a food source, and their likely



**Figure 8.** Reproduction of photograph taken by P.A. Felt of Eureka in 1877. Denver Public Library Western History Collection No. X-11438, used with permission. The view is north, up the Animas River, and shows reach A.

extermination. Beaver promote the growth of woody shrubs, which in turn promote the stability of channel banks and flood plains (Kean and Smith, 2004; Smith, 2004). We cannot evaluate the efficacy of beaver in our study area, because they were likely eradicated prior to this earliest depiction of the area. Nonetheless, thickets of willow are not apparent adjacent to the channel in figure 8. In conclusion, the channel of reach A was wide, sinuous, had low banks, and was apparently braided in 1877, if not before. The apparently braided nature of reach A is consistent with our findings in the section on implications of channel patterns, and other evidence present in the next paragraphs.

Another early photograph of Eureka (Bird, 1986, his fig. 41), attributed by Bird to have been taken in 1880, shows the channel in the upper portion of reach B as wide and braided. We were unable to locate the original print, and thus cannot confirm the date or describe the detailed character of the channel, but the tracks of the Silverton Northern Railroad are not evident, so that photograph was likely taken before 1896. The next photograph discussed (C-Eureka, 92.181.35) was found at the Colorado Historical Society archive in an album of photographs taken by the “Candee and McNutt families in 1883 and 1884.” The photograph is of people standing on the edge of the channel just downstream of Eureka. The streambed was composed of small-diameter cobbles, had vertical banks less than 1 m high, and may have been on the order of 30 m wide. The flood plain was composed of fine-grained sediment (not gravel), and was vegetated by scattered clumps of willow (about 2 m high and wide) on an otherwise barren plain that appears to have been heavily grazed. No tree stumps were visible. Currently in that viewscape of the upper portion of reach B, there are no willows, the channel is fully braided and no meter-high banks are present (fig. 2B). Evidently the upper portion of reach B aggraded since the late 1800s, burying the channel banks observed in the 1883–84 photograph.

In 1906 George L. Beam took the photograph reproduced as figure 9A, from the railroad grade looking downstream (south) at Eureka, and at our reaches A and B of the Animas River. Although Sloan and Skowronski (1975, p. 256) indicated that the photograph was taken by Beam in 1911, Thode (1989, p. 86) stated it was taken by Beam in 1906. We assume the 1906 date is correct because Thode is the acknowledged authority on George Beam and his photographs, which Thode resurrected from long-forgotten Denver and Rio Grande Railroad Company files. In any case, a photograph taken earlier from the identical viewpoint shows the same braided nature of the channels in reach A, except the channels are in slightly different locations. That photograph (labeled “Eureka” in the Silverton Northern folder of the Colorado Railroad Museum) must have been taken earlier because of the absence of the large white building that is prominent in the middle of figure 9A. Sloan and Skowronski (1975) credited the Colorado Historical Society as the source of the photograph (fig. 9A), but we have not been able to locate the original in that archive nor in the Jackson Thode collection of Beam photographs at the Colorado Railroad Museum. We reproduced

the photograph with permission from Sundance Publications (D.A. McCoy, written commun., 2004). For spatial reference, the oval-shaped patch of spruce on the hillslope in the center of the photograph, above the large white building in Eureka, is visible in the center of the left half of figure 2. The canyon of Minnie Gulch meets the Animas River valley off the center of the left margin, and the patch of spruce on the valley floor in the background is on the Minnie Gulch debris fan. In the 1999 repeat photograph (fig. 9B) the toe of the Minnie Gulch fan is located at the apex of the dogleg in the road, visible as a light stripe at center left. Our boundary between reaches B and C crosses that bend in the road (fig. 4B). This pair of photographs is important for three reasons. First, the lower portion of reach A was clearly braided in 1906. By 1999 the channel was much less braided, and appears to have incised 1 or 2 meters. In addition onsite inspection revealed the tracks of heavy machinery on the streambed in 1999. Notice in figure 9B the elevated berm of gravel on the left bank adjacent to the townsite that serves to orient the channel under the bridge. The braided pattern (fig. 9A) and the need for maintenance to protect the bridge and townsite (fig. 9B) are consistent with our findings in the section on implications of channel patterns. Second, in 1906, in the upper portion of reach B, just downstream of Eureka, the channel was wide and apparently braided or at least multi-threaded. Third, in the lower portion of reach B, approaching Minnie Gulch, wide areas of densely vegetated flood plain existed, unlike today. These observations from the 1906 photograph help interpret figure 2A, because of the tonal quality and perspective of the ca 1904 print discussed next.

The earliest photograph that shows a large extent of our study reach is reproduced as figure 2A. A print of this photograph is on file with the Colorado Historical Society (C-Eureka, F7005) but is not dated on the back. We believe that the photograph was taken in 1904, or shortly before, for two reasons. It was published in 1904 by the Silverton Standard (1904). The railroad grade leading upstream to Animas Forks is clearly visible in figure 2A, which is significant because the Silverton Northern Railroad began service to the town of Animas Forks late in 1904 (Sloan and Skowronski, 1975), and thus the photograph could not have been taken too many years before 1904. This photograph was repeated in 2001 (fig. 2B) from approximately the same site.

The following changes in the landscape between 1904 and 2001 are evident by visual comparison of the prints in figure 2. Vegetation on bedrock hillslopes and talus slopes changed very little, and certain individual spruce trees can be identified in both prints. The present road is located along the same general course as was the railroad, and these features tended to protect the east (foreground) side of the valley floor from erosion by the Animas River. Within that eastern fringe of the valley floor, the willow bushes and scattered spruce trees are only slightly less dense in the 2001 photograph (fig. 2B). In 1904 a number of large deciduous trees, presumably cottonwood, were present near the railroad. A few cottonwoods are present now. The fringe of shrubs just

west of the railroad in 1904 is essentially absent now. The band of dense (dark) shrubs and spruce along the west edge of the valley in 1904 is entirely absent now. The areas of dense shrubs might have been low terraces, or flood plain that had not been reworked in some number of centuries. The nature of the channel and flood plain varied along the central axis of the valley in 1904, but care must be taken in the interpretation (Rogers and others, 1984) because of the presence of areas in sunlight and areas of shadow in figure 2A. Just downstream of the Eureka bridge (and in the foreground of the large building with the white roof) the channel is clearly wide and multi-threaded and apparently had prominent banks. In the center of the photograph the river channel or channels are obscured, but the flood plain is occupied by sparse and small bushes that are absent now. The density and sizes of willows increase downstream in the 1904 photograph, and those plants are also absent now. At the downstream end of reach B, in the vicinity of our trench labeled T (fig. 2B), the 1904 print shows sunlight apparently reflecting off a multi-threaded stream, but the zone of channels is narrow and is bounded by flood plain covered by dense shrubs. At present, that area consists of a wide zone of shallow braided channels, and the flood plain is devoid of shrubs. The stratigraphy of the trench (pl. 6) supports the interpretation of multi-thread channels with prominent banks at that location early in the 20th century, and before, as will be discussed later.

In conclusion, reach A was braided before mining and milling became intense (figs. 8 and 9A), and was likely braided in prehistorical times. In the early days of mining, the Animas River in reach B consisted of multi-threaded channels, and the valley bottom consisted of areas of sparse willows and areas of dense vegetation. Except for the areas protected by the elevated roadbed, that entire reach is now fully braided and devoid of vegetation. The changes documented using oblique historical photographs largely occurred during the period of production of sand-sized tailings (see section on flood-plain stratigraphy), but other changes occurred after 1945, as discussed next.

## Aerial Photographs 1945 to 1997

### Methods

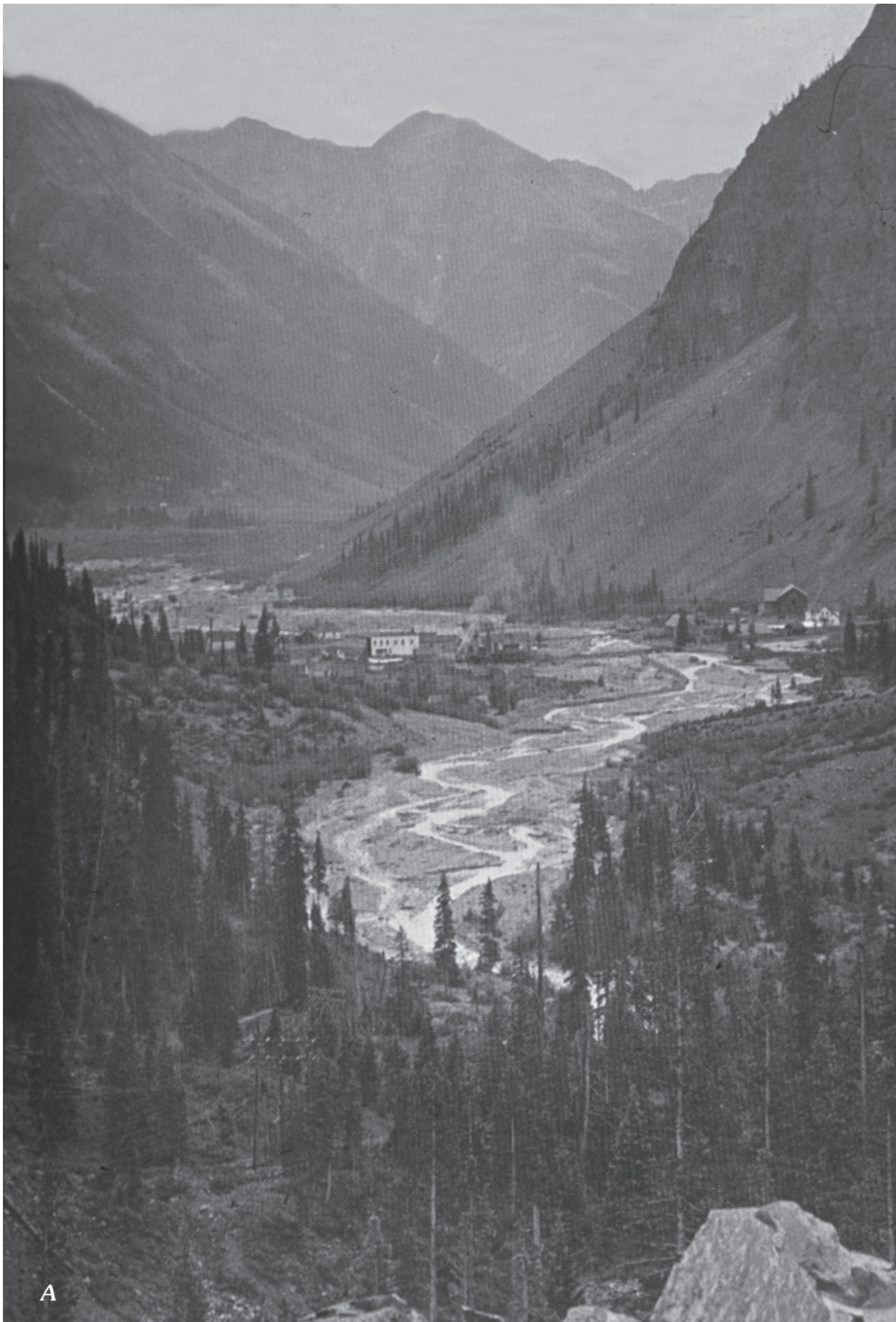
Aerial photographs of the upper Animas River valley, figure 4 for example, reveal the channel condition and position at several discrete moments in time. Examination of sets of rectified photographs allows quantification of changes in channel position and vegetation during the periods between the photograph dates (Gurnell, 1997), and is most accurately done in a Geographical Information System (GIS). Aerial photographs of the upper Animas River valley taken in 1945, 1951 (fig. 4), 1960, 1973, 1987, and 1997 were selected for that type of geomorphic analysis. Most of the photographs were taken in August or September when seasonal streamflow had receded to low levels, and the timing of the photographs with respect to the flood series is shown in table 1.

The upper Animas River aerial photographs were enlarged to 18×18 inch prints having scales of between approximately 1:6,300 and 1:14,000. The enlarged photographs were digitally scanned and these images were electronically processed to remove optical distortion and photographic parallax common to many aerial photographs. These aerial photographs were registered and rectified before geomorphic measurements and analysis were conducted. Digital image processing and geometric correction are described in greater detail by Jensen (1996). Image digital processing, rectification, and registration were done with ArcView Spatial Analyst software (Environmental Systems Research Institute, 1996).

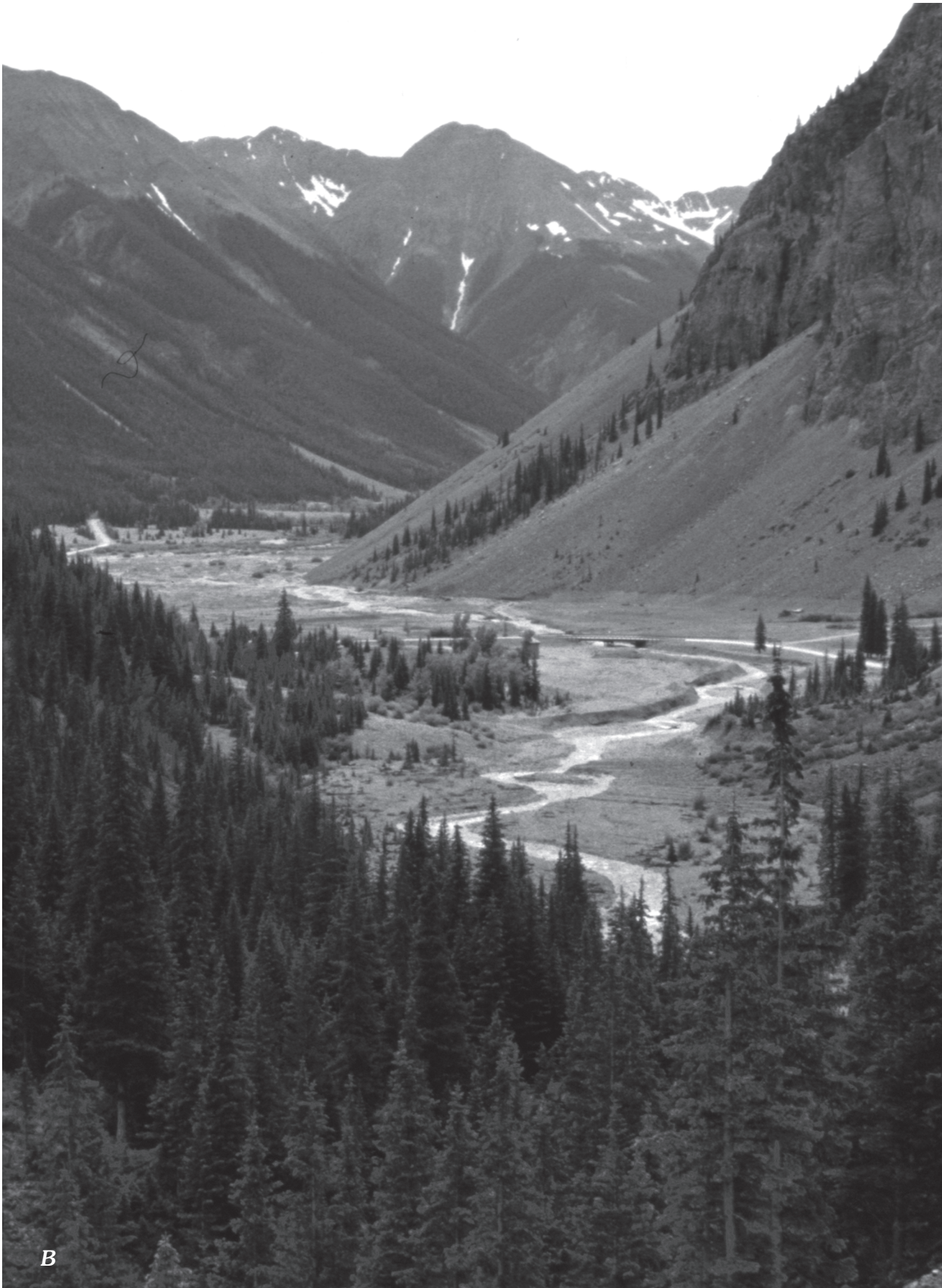
Raw, unprocessed photographs can be registered and rectified to a digital orthophoto quadrangle (DOQ) map (Elliott and Gyetvai, 1999), or they can be registered and rectified to points of known latitude and longitude. Because DOQ maps of the upper Animas River valley did not exist at the time of this analysis, two 1997 aerial photographs were rectified to 10 and 13 reference points on or near the upper Animas River flood plain using a Precision Lightweight Global-Positioning System Receiver (PLGR). Reference points were features identifiable both on the ground and in the 1997 aerial photographs, for example, railroad intersections, building foundations, road culverts, and earthen berms. Calculated PLGR latitude and longitude coordinates in the upper Animas River valley had horizontal errors ranging from 5 to 13 meters.

The rectified 1997 photographs became the standardized images to which the other aerial photograph sets were registered and rectified. Features visible in all photographs were used as rectification control points. These points were at elevations similar to the flood-plain elevation, thereby reducing the potential for rectification error caused by relief displacement (Gurnell, 1997). The unprocessed, earlier aerial photographs were rectified to the scale and coordinates of the 1997 standardized photos with second order polynomial affine transformation functions fitted to the (17 to 39) control points using a least-squares criterion (Jensen, 1996). The goodness of fit between the rectified and the 1997 standardized photo was evaluated quantitatively with root-mean-square error (RMS) statistic calculated by the ArcView Spatial Analyst extension. The RMS error describes the deviation between the control-point locations on the rectified photograph and the control-point coordinates calculated by the transformation function for the Easting and Northing directions. Table 5 presents summary statistics from the photograph rectification procedure. The RMS errors (0.83 to 2.50 m) were small (Gurnell, 1997). Consequently, we have a high degree of confidence that the apparent channel and flood-plain changes observed during

**Figure 9 (following two pages).** Photographs showing reaches A and B of the Animas River, taken from the Silverton Northern Railroad grade looking downstream at Eureka. *A*, Photograph taken in 1906 by George L. Beam, reproduced courtesy of Sundance Publications. *B*, Repeat photography by Kirk Vincent in 1999, from approximately the same location as *A*.



A



B

**Table 5.** Statistics from the digital processing and rectification of upper Animas River valley aerial photographs.

[The 1997 photographs were rectified to reference point coordinates determined in the field with a Precision Lightweight Global Positioning System Receiver. Earlier photographic images were rectified to the standardized 1997 image with a second-order polynomial affine transformation function. The term "upper reach" covers our reaches A, B, and C. "Lower reach" covers our reach D]

Photograph date and reach	Number of control points	Root mean square error, Easting (meters)	Root mean square error, Northing (meters)	Chi square, Easting	Chi square, Northing
1945 Upper reach	17	1.34	1.44	30.53	35.43
1945 Lower reach	19	1.88	1.64	66.90	51.06
1951 Upper reach	23	0.83	1.09	15.98	27.48
1951 Lower reach	19	1.60	1.49	48.68	42.00
1960 Upper reach	24	1.12	1.10	30.21	29.06
1960 Lower reach	31	1.30	1.40	52.48	60.87
1973 Upper reach	27	1.57	1.29	66.13	44.92
1973 Lower reach	39	1.13	1.13	49.77	49.79
1987 Upper reach	29	1.37	1.29	54.26	47.90
1987 Lower reach	24	1.50	1.00	53.78	23.82
1997 Upper reach	13	1.99	1.47	51.65	156.64
1997 Lower reach	10	2.50	2.00	62.44	40.09

the five photo-defined periods represent true changes on the land surface. After rectification, channel locations from all 6 years were digitized and plotted on a single map. Changes in the stream channel position and other characteristics were measured with the ArcView Spatial Analyst extension (Environmental Systems Research Institute, 1996).

We started the analysis by mapping the extent of Animas River deposits. We refer to these areas as the valley floor because they include the active streambeds, the flood plain, and any low terraces present. Operationally the boundary of the valley floor was defined as the foot of hillslopes or the toes of alluvial fans or talus cones. The intention of the valley floor map unit was to depict areas that have been or could be inundated during floods on the Animas River.

One measurement typically obtained from aerial photographs is sinuosity. Channel sinuosity is defined as the ratio of stream channel length to valley length for a specified valley segment or reach. Sinuosity is most commonly used as a descriptor of a meandering, single-thread channel; however, it also can be used to describe a property of a braided or multi-threaded channel (Richards, 1982, p. 10). In this study, we measured the normalized stream length ( $L_{ct}/L_r$ ), which is the total of all conveying channel segment lengths ( $L_{ct}$ ) visible in an aerial photograph divided by valley length of the reach ( $L_r$ ). A value of 1 would represent a single and perfectly straight channel. Larger values reflect the combined effects of the sinuosity of individual threads and, to a larger degree in this case, the total number of threads of flow. Values of  $L_{ct}/L_r$  were calculated for reaches A, B, C, and D for each aerial photograph year (table 6), and help document recent channel adjustments in the upper Animas River valley.

Channel density describes the relative abundance of channel segments per area of the valley floor. In this study, channel density is defined as the total length of conveying channels in a reach divided by the reach valley-floor area. Channel density was calculated for reaches A, B, C, and D for each aerial photograph year (table 6). A high value for channel density can occur because numerous channel threads occupy a specific area of the valley floor, as with a braided channel, or a high value can occur if there is a single channel in a laterally confined reach with a small valley-floor area. The trends in channel density match the trends in the normalized stream length ( $L_{ct}/L_r$ ), as discussed later in this section.

Riparian vegetation promotes streambank and flood-plain stability by increasing flow drag and thus decreasing boundary shear stress, by increasing bank sediment mass cohesiveness, and by inducing deposition of sediment carried in the streamflow (Thorne, 1990; Smith and Griffin, 2002; Smith, 2004). Vegetation cover and wetland areas also have important ecological functions. Valley-floor areas classified herein as either vegetated or wetland were delineated on the rectified aerial photographs from all six sets of aerial photographs, and the results are presented in table 6. These areas on the 1987 aerial photographs were field checked in 1998. Vegetated areas were covered with grasses and woody species including willow, cottonwood, and spruce, and generally had at least thin, rudimentary soils at the surface. Wetland areas were covered with willows, grasses, and sedges, or were flood-plain areas where water was impounded predominantly by beaver dams and manmade impoundments. Areas of bare fluvial sediment and actively conveying channels were excluded from either classification. The area of reach B evaluated for vegetation and wetland analysis was 67 percent of the reach B area evaluated

**Table 6.** Changes in geomorphic and wetland characteristics in reaches of the upper Animas River, from 1945 to 1997.

[Channel density,  $L_{ct}/reach\ area$ ; normalized stream length,  $L_{ct}/reach\ length$ ; nc, not calculated]

Year of photo	Total channel length ( $L_{ct}$ ) (km)	Channel density (km/km <sup>2</sup> )	Normalized stream length (km/km)	Wetland or vegetated area (km <sup>2</sup> )	Reach wetland or vegetated area (percent)	Number of beaver ponds
Reach A—"The Falls" to Eureka townsite						
1945	1.502	12.07	1.50	nc	nc	0
1951	1.384	11.12	1.38	nc	nc	0
1960	2.222	17.85	2.22	nc	nc	0
1973	2.519	20.24	2.52	nc	nc	0
1987	1.579	12.68	1.58	nc	nc	0
1997	1.443	11.60	1.44	nc	nc	0
Reach B—Eureka townsite to Minnie Gulch fan						
1945	2.875	6.57	1.95	0.0214	7.30	0
1951	4.860	11.11	3.29	.0107	3.64	0
1960	4.001	9.15	2.71	.0110	3.74	0
1973	4.292	9.81	2.91	.0125	4.27	0
1987	4.643	10.61	3.15	.0095	3.25	0
1997	6.532	14.93	4.43	.0084	2.86	0
Reach C—Minnie Gulch fan to Maggie Gulch fan						
1945	2.498	14.27	1.57	nc	nc	0
1951	2.311	13.20	1.46	nc	nc	0
1960	3.185	18.19	2.01	nc	nc	0
1973	3.214	18.36	2.03	nc	nc	0
1987	2.333	13.33	1.47	nc	nc	1
1997	2.657	15.18	1.67	nc	nc	1
Reach D—Maggie Gulch fan to Cataract Gulch fan						
1945	5.232	11.27	3.02	0.2738	58.95	4
1951	6.266	13.49	3.62	.2399	51.65	5
1960	6.617	14.25	3.83	.2446	52.66	5
1973	6.883	14.82	3.98	.2245	48.34	5
1987	4.896	10.54	2.83	.2315	49.85	14
1997	3.948	8.50	2.28	.2900	62.44	17

for channel parameter due to a large, late-day shadow that obscured part of the valley floor in the 1973 aerial photograph. That same unobscured portion of valley-floor area was used to compute wetland and vegetated areas in the other aerial photographs (table 6). The numbers of ponds evident in the photographs were counted. The ponds visible in the 1997 photographs were verified in the field in 1998 to be beaver ponds. The Forest Queen wetland in reach B has an area of open water, but it was not obvious in the aerial photographs.

## Results

During the time period represented by the aerial photograph series, the nature and position of channels and the character of the flood plain changed within individual reaches (table 6). The least change occurred in areas where the valley floor was narrow, such as at fan constrictions.

There were both spatial and temporal variations in the normalized stream length within reaches. Reaches A and C consistently had the lowest  $L_{ct}/L_r$ , and the positions of channels

were the most stable. Streamflow usually was contained in a single- or double-thread channel in reaches A and C in most years for which aerial photographs were analyzed. These reaches had the narrowest valley floors and consequently offered the least opportunity for multiple channels to develop and move. The normalized stream length values for these reaches, typically 1.5–2.0, are controlled by the sinuosity of the channels. As discussed in several sections of this chapter, however, reach A has the inherent tendency to be braided, but a single channel was maintained through use of heavy equipment. Reaches B and D had the largest  $L_{ct}/L_r$  values, typically 2.7–4, reflecting the presence of multiple channels in the reaches with the widest valley floors.

Reaches A, C, and D experienced the same pattern of changes in  $L_{ct}/L_r$  through time (table 6). In general, normalized stream length values increased during the period between years 1945 and 1973, and then decreased after that. This change may be a response (creation of threads of flow) to the large floods that occurred in 1949, 1952, 1953, and 1957 followed by natural recovery (abandonment of certain channels). Each of these floods (table 1) had recurrence interval

greater than 10 years (table 2) and generated sufficient boundary shear stresses to erode banks and transport large volumes of sediment as bed load.

Reach B had a contrasting trend:  $L_{ct}/L_r$  generally increased through the period of record—but in a complicated way. Normalized stream length was higher in 1951 than it was in 1945 or 1960, and it increased dramatically between 1987 and 1997 (table 6). The trend for this reach is unique, and it is difficult to explain in terms of a response to large floods (table 1). The actions of heavy machinery, however, are evident in the reach. For example, five manmade berms oriented perpendicular to the valley axis were conspicuous in the earliest aerial photographs of reach B (fig. 4B). They did not impound the river during the period of record. The purpose of these berms was evidently to trap tailings on their upstream sides, and they deflected streamflow eastward in the earlier aerial photographs. With time, each of these berms was breached at one or more locations and their east ends were removed, increasing the area of the valley floor that the river channels could occupy. Remnants of the berms were about 4 m high in 1998, and thus the Animas River did not cause the new breaches. Lastly, operators of the Sunnyside mine removed tailings from reach B in 1997 (Rob Robinson, Bureau of Land Management, written commun., 2004), which likely explains the unnatural ground-surface texture evident in figure 2B. These mechanical actions may have increased stream branching, and thus normalized stream length.

Data for the vegetated and wetland areas illustrate important differences between reaches B and D (table 6). Approximately 50–60 percent of the valley floor in reach D was vegetated or wetland during the period covered by the aerial photographs. In reach B, however, only 3–7 percent of the valley floor hosted vegetation or wetlands during the same period. The trend in vegetation and wetland area for reach D is almost the inverse of the trend in normalized stream length for that reach. When vegetation or wetland areas were lost in reach D, presumably due to lateral erosion accompanying the large floods in 1949, 1952, 1953, and 1957, both the length of channels and the portion of the valley floor occupied by active channels increased. Following those large floods, the vegetated and wetland area of reach D increased from 48 to 62 percent, and the normalized stream length decreased from 4.0 to 2.3 km/km, between 1973 and 1997. Part of that decrease resulted from certain channels having been turned into ponds by the action of beaver. The large flood in 1985 apparently had little adverse effect on the vegetated and wetland area calculated from the 1987 aerial photograph.

A dramatic increase in the number and size of beaver ponds in reach D was observed between the 1973 and 1987 photographs (table 6), perhaps partially reducing the flood-erosion susceptibility in this reach. These changes were not the result of introduction of beaver, as they are indigenous. For example, the growth rings of a spruce tree rooted in a relict beaver dam near Gladstone (Vincent and others, this volume, pl. 5) indicate that the tree sprouted in 1818; thus,

beaver were present in the area prior to mining. The increase in beaver habitat since the 1970s might, in part at least, be the result of reduced hunting pressure (according to a long-time resident who did not give his name). No beaver ponds were evident in reaches A and B during the study period, and the near absence of a food source may be a partial explanation. One pond appeared in the 1987 photograph of reach C.

Vegetation and wetland areas in reach B have been nearly nonexistent since at least 1945, in contrast to the vegetation cover evident in 1904 and 1906 photographs in figures 2A and 9A. There has been no recent recovery in reach B vegetation since 1987, in contrast to reach D. Almost no trees and shrubs were present along the banks of the upper Animas River in reach B when on-site measurements were made in 1998 or in 2001 when the photograph of figure 2B was taken. The lack of vegetation recovery in reach B could be explained in several ways. The vast expanse of gravel may simply be an unsuitable substrate for rapid colonization of willow in this high-altitude setting. The floods of 1949, 1952, 1953, and 1957 (fig. 2) may have removed some emergent vegetation in reach B, and the actions of heavy machinery may have done the same. Large areas of tailings beds were evident in the photographs, and these beds may have inhibited the growth of young willows in those locations by either physical or chemical processes. The extent of those tailings beds decreased through time, however, as discussed in a later section. For example, 40 percent of the light-colored tailings visible in the 1951 photograph (fig. 4B) had been removed, presumably by the action of floods, by the time the 1960 photographs were taken. Yet tailings remain in the interstices of the gravel, as demonstrated in a later section. The presence of tailings in the gravel may have contributed to the absence of willow recruitment by some chemical processes, although that possibility has not been tested directly.

## Changes Inferred from Flood-Plain Stratigraphy

We excavated a trench (pl. 6) across the alluvial valley bottom in order to understand from a stratigraphic point of view the following: the prehistorical nature of the Animas River, the historical changes in that system, and the chemistry of fine-grained sediment deposited in the distant and recent past. The location of the trench was at the downstream end of reach B, as indicated in figures 1, 2, 3, and 4B.

The trench was excavated using a trackhoe in September of 1998. For practical reasons the trench was excavated and studied in “skip sections” (fig. 10), such that short (10–30 m long) sections of the transect were excavated, studied, and backfilled. Then the intervening sections were excavated to complete the stratigraphic log of plate 6. One reason that the trenching was feasible is that the water table of the shallow alluvial aquifer was on average 1.5 m below the streambed at the time of excavation (fig. 10). An electric pump connected



**Figure 10.** Photograph of a section of the stratigraphic trench (near 156 m on pl. 6), showing the ground-water table 1.6 m below the level of that thread of the stream in late September 1998. View is looking east down the trench transect, with Colorado State road 110 visible in the background. The trench was located at the downstream end of reach B, as indicated in figures 1 through 4.

to a portable generator was used to temporarily lower the water table in trench sections, which allowed us a short time to view and sample the deeper sediment. Our depiction of the stratigraphy beneath the water table on plate 6 is therefore less reliable than that above the water table, which was available for inspection for many days.

Figure 10 is an appropriate vehicle for starting the discussion of the valley bottom stratigraphy for several reasons. The ground-water table was below the level of (and thus disconnected from) the stream during that period of late-season base-flow conditions. In late July 1998 the water table was observed to be about 1 m below the ground surface in a test pit (at horizontal distance 187 m, pl. 6), and 2 months later it had dropped to about 2.2 m below the ground surface at that location when the trench was excavated. The water in the stream was not infiltrating, and thus not recharging the shallow ground water in a significant way, because the streambed was completely coated and sealed by an algal mat. The algal mat evidently formed during the summer because the streambed had no shade. The mat was also fragile. After the trackhoe rolled over a channel (shown at 275 m on plate 6) one time, all of the stream water in the channel abruptly drained into the subsurface. Understanding the connection or disconnection of surface water and shallow ground water is essential to tracer dilution studies such as that of Kimball and others (this volume). They did not detect a gain in discharge within the braided reach upstream of the trench during their August 1998 tracer dilution study, which is consistent with our field observation of the surface water/ground water disconnection.

The foreground of figure 10 also illustrates the weak stratification typical of the gravel deposits, and that the pebbles and cobbles were subangular to subrounded. That rounding of the edges of clasts was the result of abrasion by natural stream processes through time. We mention this to indicate that the origin of these clasts was not the result of blasting of bedrock or milling of ore. In the middle left of the photograph, a vertical bank of dark gravel with an orange layer was exposed, illustrating the discoloration and cementation of gravel by iron (orange) and iron/manganese (dark) secondary salts that were common in the stratigraphic section. Much of that cementation must have occurred in the past century or less. In the background were several large relict willow bushes. These appear similar to the clumps of willow observed in the 1883–84 photograph, and in the 1904 photograph of figure 2A.

## Stratigraphy and Sedimentology

The trench was excavated perpendicular to streamflow and extended nearly the full width of the alluvial valley bottom. The only areas not excavated were the two main channels, Colorado State road 110, and short sections of flood plain at the extreme east and west sides of the valley. The trench face was 297 m long and exposed 607 m<sup>2</sup> of sediment in the trench wall (pl. 6). Four sedimentary facies were present, and their

spatial extents are discussed next in percents of the total area of the exposure. Those sediments consisted of (1) sandy gravel deposits (83 percent), (2) dark-brown silt beds (12.6 percent) containing minor amounts of peat, (3) lenses and tabular beds of sand-sized tailings (1.2 percent), and (4) tabular beds of fine-grained tailings (3.2 percent). The gravel facies represents sediment transported as bed load and deposited on the streambed, and the brown silt beds represent sediment carried in suspension and deposited on the flood plain. These deposits are discussed in terms of their stratigraphic position, low to high elevation in the section, and thus in terms of general age from oldest to youngest.

The base of the section was dominated by sandy gravel deposits. These gravels locally contained (1) discontinuous parallel bedding usually inclined less than 5°, (2) medium, curved, parallel, trough crossbedding, (3) sixteen lenticular (two were tabular) beds of brown sandy silt between 5 and 60 cm thick and less than 3 m in length, and (4) tabular or irregular-shaped beds of silty to gravelly sand.

The elevational middle of the section consisted of extensive silt beds separated laterally by gravel deposits. Eight thick beds of dark-brown (10YR 4/3 moist, 5/3 dry) sandy silt were present in the section. The color names (such as dark brown) and color codes (such as 10YR 4/3) used herein are standardized technical descriptions (Munsell Color, 2000) determined using soil color charts. These large silt beds were from 20 to 170 cm thick, ranged in length from 4 to 25 m, and spanned about 30 percent of the trench length. The bases of the silt beds were generally in planar-horizontal contact with underlying gravel, but lenticular or wedge-shaped silts also interfingered with underlying gravel. The silt beds contained (1) lenses of gravel, (2) a few lenses of peat (as much as 5 cm thick and less than 3 m long), (3) fourteen peat lamina (1 cm thick and 1–10 m long), (4) leaves and root casts possibly left by grasses, and (5) abundant twigs (presumably willow) some of which were in growth position. One twig was obviously chewed by a large mammal, possibly a beaver. Aside from those features, the silt beds appeared from a distance to be uniform and without sedimentary structures. Close inspection, however, indicated that the silt beds also contained very thin lenses of fine sand, irregular-shaped bands of climbing ripples composed of coarse silt, and 10-cm deep indentation markings left by large mammal hooves. The silt beds were either overlain conformably or were truncated by wavy or irregular erosional surfaces.

Also in the elevational middle of the section, channel-fill gravel deposits truncated the lateral extent of the thick silt beds at several locations. The former stream banks composed of silt were about 1 m high. The channel-fill deposits consisted of sandy gravel that contained (1) discontinuous parallel bedding, (2) medium, curved, parallel, trough crossbedding, (3) and lenticular or irregular-shaped deposits of coarse sand 10–40 cm thick. Nine of the sand lenses were dominated by angular grains of sulfide or gangue minerals (sphalerite, pyroxmangite, and pyrite); two of these lenses contained historical iron objects. The surfaces of pyroxmangite crystals were still pink, which is important because pyroxmangite darkens rapidly

when exposed to oxygen. We inferred that these were deposits of stamp-mill tailings, and they ranged in size from medium sand to granule (0.25–4 mm).

The upper meter of the section consisted of sheets of sandy gravel and extensive beds of fine-grained tailings. The gravels were either horizontally bedded or trough crossbedded. These gravels contained lenses and two beds (10–40 cm thick and 3–11 m long) of coarse tailings, and numerous historical artifacts including sawn lumber and metal objects. The sheet gravels were exposed at the surface for about half the length of the trench. Elsewhere the surface consisted of extensive tabular beds of fine-grained tailings typically 10–50 cm thick. The beds of fine-grained tailings were generally without obvious sedimentary structures, but locally contained crossbedded laminations, and climbing ripples suggesting deposition from suspension. Although generally composed of silt-sized particles, the tailings also contained very fine sand and clay-sized particles. The colors of the fine-grained tailings were variable, but so unusual and vivid that they were diagnostic (fig. 11). The beds were typically white (10YR 8/2) or yellowish brown (7.5YR 5/9 to 10YR 5/8), and occasionally olive (5YR 5/3), where observed in fresh exposures. Where undisturbed, however, the surface of the tailings deposits was consistently colored light olive gray (5Y 6/2).

Locally the gravel and sand deposits were stained or cemented by compounds of manganese and iron (fig. 10; pl. 6). Typically the coatings and cement were bluish black (SPB 2.5/1) in color. The cemented or discolored zones were irregular in shape, with the only generalities being they were typically laterally elongate and the tops of the zones were usually located from 0.5 to 1 m below the ground surface. The bottoms of zones were located as much as 1 m above the ground-water surface (as it was at the time of trenching), or extended down to or beneath the ground-water surface. Thus the zones were generally restricted to within the elevation range of annual fluctuations of the water table. The boundaries of the cemented or discolored zones were not restricted to changes in hydraulic conductivity of the host sediment. Locally the boundaries conformed to stratigraphic contacts or internal bedding, but locally the boundaries also crosscut stratification or ended within a bed. The cementing compounds were precipitated from the alluvial ground water after deposition of the host gravel, much of which is historical in age. A portion of the surface of the gravel flood plain was also locally bluish black in color, as indicated on plate 6. In those locations the tops of surficial stones had continuous, 1-mm thick varnish-like coatings, which evidently precipitated from stream water or temporarily ponded water. These blackened gravel bars were evident in the 1945 aerial photographs.

### Constraints on Ages of Sediment Deposition

Four types of evidence (historical artifacts, radiocarbon dating, willow growth rings, and photographs) were used to constrain the depositional ages of deposits exposed in the trench (pl. 6), and retrieved from a hole augered into the

nearby Forest Queen wetland. That wetland is located on the east side of the valley floor, just downstream from the trench, and is discussed by Stanton, Fey, and others (this volume, Chapter E25) and Finger and others (this volume, Chapter F).

Numerous historical artifacts were discovered in the trench wall (pl. 6), in the middle and upper (elevation) portions of the exposed stratigraphy. These artifacts include iron objects (cans, pots, barrel hoops, and a stove leg), cloth fabric, sawn lumber, porcelain fragments, a rubber machinery belt, and a brick. We could not determine a refined manufacturing-age for any of these objects, but we can constrain when they were introduced to the area. We conclude that the sediment containing any historical artifact was deposited after 1871 and probably after 1899 when the first mill was constructed in Eureka. The tailings are like historical artifacts in that we know when they were manufactured, and that is also when they were introduced to the fluvial system. The coarse-grained stamp-mill tailings were first produced in 1888; quantities increased and began being discharged adjacent to the Animas River starting in 1900. The use of stamp mills ended in 1918, but the tailings became increasingly finer as new technology was employed. For example, Jones (this volume) suggests that the “Gravity Milling era” ended in 1913, so we use that date for the end of, or diminished rate of, production of coarse tailings. The fine-grained tailings were produced between 1913 and 1930. Like any artifact, the age of tailings deposits must be younger than when the material was first produced or introduced to the area. The tailings, particularly the coarse-grained tailings, may have resided elsewhere in the landscape for a long or short period of time before being transported and deposited at what became the trench site.

The gravel bars blackened by compounds of manganese and iron (discussed in the preceding section) are evident in the 1945 aerial photographs. Thus gravel aggradation ceased before 1945 at those specific sites, if not in general.

Important age constraints were derived from a pair of willows that had been pushed over by flood waters, covered by sediment, and subsequently resprouted. This occurred repeatedly, and one of the plants is illustrated in figure 12. The plants were discovered alive and recently exhumed and exposed in a streambank 100 m downstream of the trench site. The stratigraphy at that site consisted of three gravel beds (labeled G1 to G3) covered by a stratified bed of fine-grained tailings (labeled T). The tailings are thicker on the downstream side of the plant (fig. 12) than on the upstream side. Analysis of plant growth rings has long been used to determine the timing of tissue damage (scarring or bending) or burial, and thus the age of causal events such as floods. (See, for example, Sigafos, 1964; Scott and others, 1997.) Mike Scott of the USGS analyzed the growth rings of 10 slabs cut from the two willow plants (written commun., 1999) allowing the following conclusions to be made. The willow shown in figure 12 sprouted in 1915 ( $\pm 3$  years) on a gravel bar close to the present level of the stream. Thus the gravel at the base of the section (G1) was deposited before that, perhaps



**Figure 11.** Fresh exposure of flood-plain sediment located near the trench site. The base of the 1-m high exposure was composed of dark-brown sandy silt. The middle of the exposure was composed of sandy silt containing very thin beds of fine-grained tailings. The top of the exposure was composed of thin to medium-thick beds of yellowish-brown, white, and olive-colored fine-grained tailings.



**Figure 12.** Recently exposed willow bush that had been repeatedly pushed over and covered by sediment, only to resprout. Labeled dates are based on growth-ring analysis discussed in text. Willow was located about 100 m downstream of the trench (pl. 6).

during the 1911 flood of record. The previously undisturbed plant stems were permanently bent downstream around 1920; thus, gravel bed G2 may have been deposited during the 1921 flood that is known to have caused damage in the area. Plant tissue from within gravel bed G3 showed signs of burial by 1929; thus, bed G3 may have been deposited during the large 1927 flood recorded at the Durango gauge. The aggradation of gravel at the site occurred during or shortly after the introduction of large quantities of coarse-grained tailings, and perhaps coincidentally during the period of huge production of fine-grained tailings (fig. 7). Willow stems showed signs of slowed growth caused by some disturbance around 1941, 1949, possibly in the late 1950s, between 1970 and 1974, and during the first half of the 1980s. Thus the fine-grained tailings shown in figure 12 may have been deposited from suspension during the floods of 1949, 1957, 1973, and 1985. One other disturbance must be accounted for. At some point lateral migration of the stream, or incision, exhumed and presumably stressed the plants; this may have occurred during the 1973 or 1985 floods.

Select twigs and peat samples were dated using standard radiocarbon techniques (data are presented in table 7). The results appear graphically in figure 13 and are discussed in the next section.

## Stratigraphic Interpretations

The oldest dated sediments are under the Forest Queen wetland on the east side of the valley. Peat obtained from a depth of nearly 5 m below the surface is slightly more than 3,000 years old (fig. 13). Since that time sediment in the spring-fed wetland accumulated at the average rate of 1.5 m/ka (meter per thousand years), with rates ranging from 0.8 to 3.4 m/ka. These rates were calculated using calibrated radiocarbon ages (table 7). The rates were slowest (0.8 and 1.1 m/ka) in the lowest 2 m of the section, perhaps in part due to compaction of those sediments. These rates are fairly rapid compared to other prehistorical rates of aggradation, based on measurements made in the area. For example, Carrara and others (1991) determined that several bogs in the area aggraded about 0.2 m/ka through the early and middle Holocene. Vincent and others (this volume) determined that peat wetlands on the flood plain of Cement Creek aggraded at rates on the order of 0.5 m/ka during the late Holocene. Vincent and others (this volume) also determined that the channel of Cement Creek aggraded as rapidly as 1.7 m/ka during the late Holocene. Three dates of about 1,100 years were obtained by this study from a depth of about 2 m below the present flood-plain level (fig. 13), but approximately 1 m of that overlying sediment is historical in age. The average prehistorical aggradation rate for the Animas River and flood plain is thus on the order of 1 m/ka. These rates pale in comparison to that for the historical period, when more than a meter of sediment accumulated over several decades.

Extensive gravel deposits dominate the base of the stratigraphic section exposed in the trench. We interpreted this to represent a period of deposition and reworking by broad braided streams, with only localized deposition (or preservation) of fine-grained flood-plain deposits. This period apparently ended about a thousand years ago.

Two changes in the landscape are evident in the middle of the stratigraphic section. After 1,000 or 2,000 years ago, the brown silt flood-plain deposits began to accumulate (and were preserved) in between multiple channels of the Animas River at the trench site. The flood plain likely consisted of dense thickets of willow and areas of grasses between sparse willow bushes. The thin layers of peat within the silt beds suggest that beaver ponds were locally or occasionally present on the flood plain. This period of multi-threaded channels surrounded by vegetated flood plain persisted until the early 20th century, based on the observations made from early historical photographs discussed previously. The existence of the multi-threaded channels evident in the ca 1904 photograph (fig. 2A), in particular, supports the stratigraphic interpretation of the nature of channels and flood plain. That general timing, of the development of the silty flood plain, is consistent with the results of the better dated study of Cement Creek (Vincent and others, this volume). Cement Creek was apparently not aggrading between about 6,000 and 1,500 years B.P., after which both the channel and flood plain began to aggrade. About 500 years B.P., Cement Creek incised 2–3 m, but if the Animas River in our study area incised at that time it was only by a small amount.

Rapid changes in the upper Animas River valley occurred during historical times. The channels were filled with gravel, broad sheets of gravel were deposited on the flood plain, and then fine-grained tailings were deposited over much of the valley floor at the trench site. The deepest stamp mill tailings (at 34 and 44 m on pl. 6) may have been deposited late in the 19th century or early in the 20th century, before rapid channel filling began. The two large beds of stamp-mill tailings (between 44 and 53 m, and between 87 and 99 m on pl. 6) were deposited on the flood plain before the channels were full of gravel, based on crosscutting relationships at the margins of the beds. This likely occurred after 1900, because only a modest quantity of tailings was produced before that (fig. 7). Channels at the trench site were not full of gravel in 1904 (fig. 2A). The channels may have been partially filled with gravel during the 1911 flood, but this cannot be demonstrated conclusively. At the site of the dated willows (fig. 12) 100 m downstream of the trench, gravel at the base of the section was likely deposited in 1911, but the bulk of the streambed gravel was probably deposited during the 1921 and 1927 floods. Much of the gravel accumulation in the reach at the trench also likely occurred in the 1920s. The 1945 aerial photograph shows broad sheets of blackened gravel and also tailings at the trench site; thus, the period of rapid aggradation ended before that time. After 1945, the surficial tailings beds were locally reworked and transported downstream, as discussed in a later section of this chapter.

**Table 7.** Data for radiocarbon samples collected near the trench, downstream of the Eureka townsite.

[Note that "B.C." and "A.D." are both placed before dates in this table, for better readability and quicker recognition]

Field No.	Lab No.	Material	$\delta^{13}\text{C}$ per mil	$^{14}\text{C}$ age <sup>1</sup> years B.P.	Calibrated ages <sup>2</sup>			Distance along trench, m
					Intercept (s) <sup>3</sup>	1-sigma range <sup>4</sup>	2-sigma range <sup>4</sup>	
Samples from core in wetland at the Forest Queen mine								
AVT-A2-1.5	GX-24744-AMS	wood	-25.8	930±50	A.D. 1040–1160	A.D. 1020–1180	A.D. 1000–1220	( <sup>6</sup> )
AVT-A2-2.85	GX-24746	peat	-27.3	1,220±75	A.D. 780	A.D. 690–890	A.D. 660–990	( <sup>6</sup> )
AVT-A2-4.1	GX-24745	peat	-28.0	2,305±70	B.C. 390	B.C. 400–230	B.C. 540–180	( <sup>6</sup> )
AVT-A2-4.85	GX-24743	peat and wood	-26.5	3,020±90	B.C. 1290–1260	B.C. 1400–1130	B.C. 1490–1000	( <sup>6</sup> )
Samples from the flood-plain trench (pl.6) downstream of Eureka								
AVT-65.2-0.9	GX-25027	wood	-26.6	Modern (102%) <sup>5</sup>				65.2
AVT-93-0.93	GX-24741	peat and twigs	-25.1	Modern (102%) <sup>5</sup>				93
AVT-69-2.2	GX-24739	wood	-23.2	1,080±120	A.D. 980	A.D. 780–1030	A.D. 680–1220	69
AVT-127-2.3	GX-24742-AMS	charcoal	-22.2	1,210±60	A.D. 780–800	A.D. 690–890	A.D. 670–980	127
AVT-92-1.25	GX-24740	peat	-25.5	2,130±145	B.C. 170	B.C. 380–A.D. 50	B.C. 480–A.D. 210	92

<sup>1</sup>Conventional radiocarbon age ( $\delta^{13}\text{C}$  corrected), based on the Libby half life (5,570 years) for  $^{14}\text{C}$ , as reported by Geochron laboratories in years before A.D. 1950 (years B.P.). Sample analyses done using accelerator mass spectrometry denoted with the letters AMS in the lab number. The error is  $\pm 1$  sigma as judged by the analytical data alone. The sample was crushed if necessary and dispersed in water. The eluted clay/organic fraction was treated in hot dilute IN HCl to remove any carbonates. It was then filtered, washed, dried, and combusted in oxygen to recover carbon dioxide for analysis.

<sup>2</sup>Ages calibrated using the CALIB4.3 program based on Stuiver and Reimer (1993) with data from Stuiver and Braziunas (1993) and Stuiver and others (1998). The 1998 atmospheric decadal data set and laboratory error multiplier  $K=1$  were used in the calculations.

<sup>3</sup>Maximum and minimum values given if the radiocarbon age intercepted the calibration curve at multiple locations. Age(s) rounded to the nearest decade if the standard deviation in the radiocarbon age was  $\geq 50$  years.

<sup>4</sup>Calibrated age range (or the maximum and minimum if there was more than one range) using the intercept method. Ages rounded to the nearest decade if the standard deviation in the radiocarbon age was  $\geq 50$  years. 1 sigma = square root of (sample standard deviation<sup>2</sup> + curve standard deviation<sup>2</sup>); 2 sigma =  $2 \times$  square root of (sample standard deviation<sup>2</sup> + curve standard deviation<sup>2</sup>).

<sup>5</sup>Sample with "modern" age had the given percentage of the A.D. 1950  $^{14}\text{C}$  activity, and is considered younger than A.D. 1850.

<sup>6</sup>From Forest Queen site (fig. 13). Samples not on trench transect.

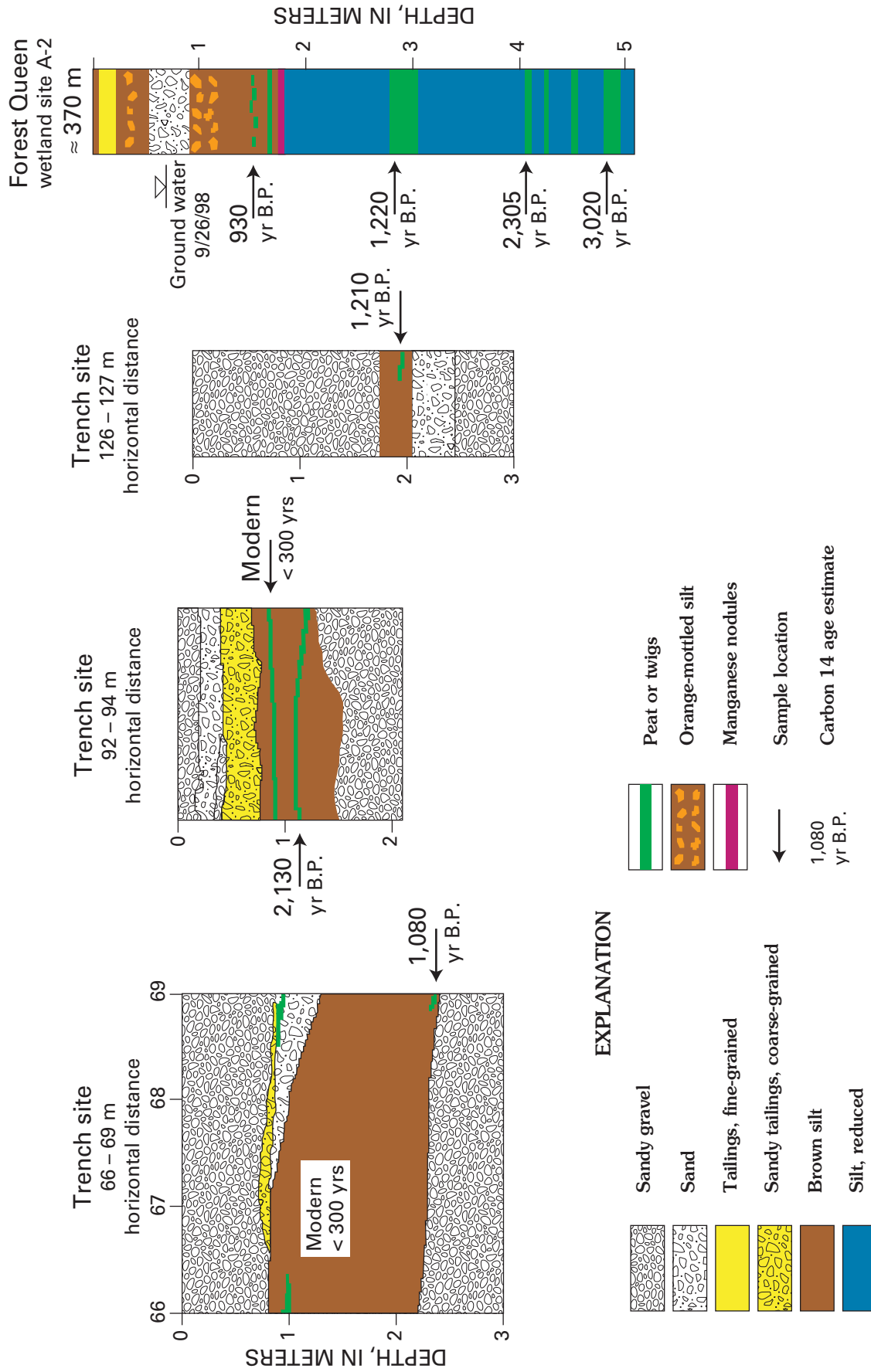


Figure 13. Summary of dated stratigraphy of the Animas River valley flood plain near the trench site (pl. 6).

## Sediment Chemistry

In order to understand the chemistry of sediment deposited in the distant and recent past, we obtained and analyzed 82 samples of sediment. These were extracted from the trench wall or obtained from cores of tailings and silt beds adjacent to the trench.

## Geochemical Methods and Results

The sediment samples extracted from the trench wall were generally about 1 L (liter) in volume, whereas samples from cores were somewhat smaller. Four 5-cm diameter cores, each approximately 1 m long, were taken adjacent to the trench. The cores were subsequently divided at visual changes in mineralogy or sedimentology into from 4 to 12 subsamples, with typical volumes of 50 cm<sup>3</sup> (cubic centimeters).

Sample preparation and geochemical analysis followed the methods used by Fey and others (2000) in their regional study of the geochemistry of sediment in the Animas River watershed. All samples containing gravel were passed through a stainless steel sieve with 2 mm mesh opening, and the gravel clasts were discarded. All samples were air dried, and sieved to -100 mesh (<0.15 mm), and then crushed to -150 mesh (<0.1 mm), except for the early stamp-mill tailings, which were crushed to -150 mesh without sieving beyond 2 mm. The chemistry was thus determined for very fine sand, silt, and clay-sized particles in the samples of silt beds, fine-grained tailings, and sandy gravel. For the stamp-mill tailings samples, only, the chemistry of the coarse sand and finer particles (<2.0 mm) was determined. The analytical results are therefore representative of the entire volume of brown silt beds and tailings deposits, but representative of only the fine fraction (<0.15 mm) of the sandy gravel samples.

After grinding, all samples were digested using a mixed-acid procedure (Briggs, 1996). This procedure is very effective in dissolving most minerals, including silicates, oxides, and sulfides. Some refractory minerals such as zircon, chromite, and tin oxides are only partially attacked; however, elements contained in these minerals were not of concern in this study. The resulting solutions were analyzed by inductively coupled plasma-atomic emission spectrometry (ICP-AES) for major elements and trace elements. To monitor the quality of analyses, laboratory duplicates were analyzed to assess precision, and three standard reference materials were analyzed with the sample sets to assess analytical accuracy. The reference materials were NIST-2704, NIST-2709, and NIST-2711, available from the National Institute of Standards and Technology (NIST, 1993a, 1993b, 1993c). We discuss here results for zinc and vanadium, but all analytical results are found in the database of Sole and others (this volume, Chapter G).

In order to establish the trends in element concentrations in the streambed and flood-plain sediment, we ranked all samples by their stratigraphic position (relative age) using the trench log of plate 6. The horizontal axis of figure 14A

and B reflects that ranking. The <sup>14</sup>C ages allowed identification of those sediments that were definitely deposited before the mining era (fig. 14C). The age constraints provided by the presence of tailings and historical artifacts, and the growth rings of willows, allowed identification of those sediments that were definitely deposited after milling began (fig. 14C). The geochemical data are presented using symbols for four deposit types, and the differences in the concentration of various metals in those deposit types are discussed in a few paragraphs.

The concentrations of vanadium in sediment deposited prior to mining at the trench site (fig. 14A) and elsewhere in reach B (Church, Fey, and Unruh, this volume, Chapter E12) average 140 ppm, which is close to the 160 ppm crustal abundance of vanadium (Emsley, 1991). The concentrations of vanadium in historical (post-1888) deposits average 50 ppm, in contrast. The vanadium concentrations in some of the fine-grained tailings samples are close to 20 ppm.

The concentrations of zinc in sediment (fig. 14B) deposited prior to the mining era are uniform and close to 1,000 ppm, which is an order of magnitude greater than the 75 ppm crustal abundance of zinc (Emsley, 1991). Compared to this premining background, the concentrations of zinc in most (38 out of 46 samples) of the sediment samples from material known to have been deposited after mining began are elevated by as much as 10 times.

The tailings deposits contain other metals that are substantially elevated above concentrations in sediment deposited during prehistorical times (table 8). Compared to that background, lead concentrations are elevated about 40 times in fine-grained tailings and are elevated about 20 times in coarse-grained tailings. Cadmium, copper, and manganese concentrations are elevated above background by factors between 4 and 14. In contrast, arsenic concentrations in tailings are equivalent to background. Nickel as well as vanadium concentrations are substantially less than that found in premining sediment.

In that light, the concentrations of metal in the two types of tailings are not substantially different from one another. The concentrations of zinc and cadmium are equivalent in the two tailings types. The coarse-grained tailings contain somewhat less (from 20 to 50 percent less) lead, arsenic, copper, and manganese than the fine-grained tailings.

## Geochemical Conclusions

We draw the following conclusions from these geochemical results. Sediment known to have been deposited prior to the mining era has concentrations of certain metals that are substantially elevated above concentrations typical of the Earth's crust, which is not surprising. That sediment was produced by erosion of hillslopes in the watershed, where locally the surficial bedrock contains high concentrations, even economical concentrations, of metal. The introduction of mill tailings into the fluvial system resulted in dramatic increases in concentration of certain metals (and dilution of other elements)



**Table 8.** Concentration of selected elements (in parts per million) in deposits of coarse-grained and fine-grained mill tailings.

[Samples were obtained in or near the trench (pl. 6) of this study. Data for prehistorical sediment are from Church, Fey, and Unruh (this volume, Chapter E12, sample sites B19–B23) from samples obtained within reach B. Crustal abundance values from Emsley (1991)]

Element		Deposit type		Prehistorical sediment <i>n</i> = 44	Crustal abundance
		Coarse tailings <i>n</i> = 9	Fine tailings <i>n</i> = 19		
Arsenic:	Median	40	51	55	1.5
	Mean	40	53	52	
	1 sigma	10	18	16	
	Range	28–61	28–100	23–85	
Cadmium:	Median	16	14	4	0.1
	Mean	20	15	4	
	1 sigma	12	8	4	
	Range	9–42	2–34	1–18	
Copper:	Median	1,500	2,000	120	50
	Mean	1,390	1,990	142	
	1 sigma	454	720	67	
	Range	530–2,000	760–3,100	92–480	
Lead:	Median	7,800	14,000	360	14
	Mean	7,756	16,900	403	
	1 sigma	3,085	13,700	212	
	Range	3,800–14,000	5,500–65,000	150–1,600	
Manganese:	Median	28,000	35,000	3,700	950
	Mean	27,778	33,632	4,448	
	1 sigma	4,295	10,084	1,737	
	Range	22,000–34,000	13,000–47,000	2,500–9,100	
Nickel:	Median	7	4	14	80
	Mean	6	5	14	
	1 sigma	2	2	3	
	Range	3–8	2–8	9–20	
Vanadium:	Median	64	38	140	160
	Mean	56	40	135	
	1 sigma	17	20	12	
	Range	30–78	12–77	120–160	
Zinc:	Median	3,200	4,500	940	75
	Mean	4,411	4,585	1,022	
	1 sigma	3,209	2,437	258	
	Range	1,300–10,000	920–10,000	720–1,800	

in historical sediment compared to the premining background sediment at the trench site (Vincent and others, 1999), and at sites downstream (Church, Fey, and Unruh, this volume).

The trend in zinc concentration shows a dramatic increase, by as much as 10 times (fig. 14B). This increase occurred both in sediment deposited in streambeds and bars, and in sediment deposited on brush-covered flood plains. The concentrations of zinc in sediment known to have been deposited prior to the mining era are uniform and close to 1,000 ppm. The concentrations of zinc are also close to 1,000 ppm in most (all but four) of the samples whose depositional ages are uncertain relative to the beginning of mining and milling (fig. 14B). The concentrations of zinc are elevated, however, in most (38 of 46 samples) of the samples of sediment known to have been deposited after mining began, and more specifically after mill processing of ore began in earnest.

We infer, therefore, that the increase in zinc concentrations in streambed and flood-plain sediment was caused by the release of huge quantities of tailings from the mills, most notably the Sunnyside Eureka Mill (site # 164).

The trend in vanadium concentration is opposite to that for zinc (fig. 14A). The vanadium concentrations in premining sediment are similar to that typical of the Earth's crust. In contrast, they are also, in general, three times higher than the concentrations in historical deposits. Mining did not cause an increase in the release of vanadium to the environment; rather it diluted the premining vanadium concentration with mill tailings. We conclude that vanadium can be used as a lithologic tracer for sediment derived from premining erosion of the watershed. The average vanadium concentration is 23 ppm, for the 10 tailings samples with the lowest values (out of 28), and we assume this is representative of pure tailings. The

average vanadium concentration for the fine-grained fraction of premining gravel samples is 135 ppm, and is 60 ppm for that of historical gravel samples at the trench. Using a simple mixing equation, we conclude that the fine-grained fraction of historical sediment at the trench site is, in general, composed of two-thirds mill tailings and one-third premining sediment unrelated to mining or milling. This proportional tailings content is, if anything, an underestimate. Using a value larger than 23 ppm for the vanadium concentration of pure tailings would result in a larger estimate of the proportional tailings content. Given the way we use this mixing result in the section titled, "Current Location of Tailings," however, we consider this estimate (two-thirds of the fine fraction is tailings) to be conservative.

The concentration of lead in fine-grained tailings is 16,900 ppm, substantially higher than the 7,760 ppm for coarse-grained tailings (table 8). We conclude that lead can be used as a lithologic tracer for determining the provenance, and manufacturing age, of tailings. For example, the ratio of lead and vanadium concentrations is about 3 for premining sediment. The ratio of lead and vanadium concentrations is about 140 for the older coarse-grained tailings, whereas it is about 420 for the younger fine-grained tailings.

The concentrations of other metals in the two types of tailings are not substantially different from one another (table 8). The concentrations of copper, manganese, and zinc are somewhat higher in fine-grained tailings compared to that in coarse-grained tailings. More important, however, is the surface area of mineral grains available for geochemical reactions, per unit volume or mass of sediment, which depends on particle size. For example, silt-sized particles have about 100 times more surface area (per unit mass) compared to medium sand (Birkeland, 1984). The fine-grained tailings are dominated by silt-sized particles and should be more reactive, compared to the coarse-grained tailings dominated by sand. In addition, most of the fine-grained tailings reside at the ground surface and thus are easily accessible, whereas most of the coarse-grained tailings reside in the subsurface. For that reason it might be prudent to base decisions for prioritizing mitigation of the two types of tailings on factors other than differences in chemistry.

## Current Location of Tailings

The desire to remove mill tailings from the landscape for environmental reasons has been expressed. The environmental concern is that metal may be extracted from the sediment by geochemical processes and transported by water. That water may enter streams where the metal may have an adverse effect on aquatic life, or enter plants where the metal may have an adverse effect on wildlife using the plants as a food source. Although discussion of geochemical processes is beyond the scope of this project, the presence of tailings within stream sediment may result in increased metal concentrations in local

water. Indeed the Animas River in our study area does have elevated zinc concentrations, comparable to that in Cement and Mineral Creeks (Kimball and others, this volume). Therefore, we discuss where the tailings currently reside in the study reach, and how that has changed through time. The tailings reside in the landscape at the ground surface and in the subsurface, and these two deposit types need to be discussed separately, for practical reasons.

Beds of fine-grained tailings at the ground surface can be remediated relatively easily and efficiently, for three reasons. These beds of tailings are easy to identify because of their unique colors (fig. 11), and they are easy to excavate because they are at the surface. They can also be efficiently processed because they do not contain gravel clasts, which otherwise would presumably be separated from the tailings before shipment to a repository. The owners of the Sunnyside mine removed most of the surficial beds of tailings in reach B, proving the viability of remediation of that deposit type. In addition, unless those deposits are reclaimed, they are to some degree susceptible to being mobilized by streamflow and flushed downstream to be deposited in dilute form in inaccessible locations, as discussed next.

The spatial extent of beds of fine-grained tailings (table 9) was interpreted using the aerial photographs discussed previously, based on the gray tone and smooth texture of the ground surface typical of those beds. For an example see figure 4. The extent of tailings in 1945 was not interpreted because of the poor tonal quality of that photograph set. Tailings deposition was most extensive closest to the source mills in Eureka, namely in reach B. The apparent extent of tailings beds in reach D was and is relatively minor. The extent of the tailings beds decreased dramatically through time, in reaches B and C. Of the tailings present in 1951, by 1960 about 40 percent disappeared from reach B, and about a third disappeared from reach C (table 9). We presume that was largely the result of the three large floods that occurred in the 1950s (table 1). Between 1960 and 1987 the areas of tailings in reaches B and C continued to decrease, but at a less dramatic rate; and we attribute these changes to the actions of streamflow, which mobilized the fine-grained tailings and largely transported them out of the study reach. The decrease in reach B between 1987 and 1997, however, is attributed to the remediation actions of the owners of the Sunnyside mine.

**Table 9.** Spatial extent of surficial fine-grained tailings as interpreted from aerial photographs, by reach and year.

Reach--	B	C	D
Date	Area of tailings, square kilometers		
1951	0.23	0.06	0.01
1960	.14	.04	.02
1973	.13	.04	.01
1987	.09	.03	.01
1997	.03	.02	.00

In conclusion, streamflow has mobilized and exported tailings from the study area and will continue to do so. This is not without consequences. Church, Fey, and Unruh (this volume) studied the chemistry of streambed sediment at many locations along the Animas River. They demonstrated that stream sediment deposited in historical times contains elevated concentrations of several metals, compared to sediment deposited in prehistorical times. Just as we have done in this study, they attributed the elevated metal concentrations to the presence of mill tailings within the historical stream sediment. The geochemical signature of tailings is present in stream sediment at least as far downstream as Durango, Colo. The rate of export of tailings from the study area by streams, however, should be much slower in the future than it has been in the past, for two reasons. First, the extent of fine-grained tailings is currently much less than it was previously (table 9). Second, the remaining beds of fine-grained tailings reside at elevated sites, or are otherwise protected from common streamflows. In a previous section, we estimated the discharge needed to begin to inundate the tailings beds observed at the trench (pl. 6). The result was a discharge of 42 m<sup>3</sup>/s, which is a rare discharge according to the measurements made at the Howardsville stream gauge (tables 1 and 2). As an annual instantaneous peak at that gauge, this discharge has a recurrence interval of about 10 years (table 2). The tailings beds could be locally mobilized by lateral migration of channels, as well as by flood inundation, but the calculation illustrates that the remaining tailings beds are relatively protected from erosion.

The coarse-grained tailings residing in the subsurface are even more protected from stream erosion, and remediation of that material would be an involved process. Relatively pure beds of tailings occur in the subsurface, but they are thin and are discontinuous, and their locations cannot be predicted accurately. For example, Campbell and Eckhart (2000) conducted geoelectrical studies along the trench transect just before the trench was excavated. They measured the local magnetic field and the electric conductivity and polarizability of the ground, and they did a ground-penetrating radar survey. The results were compared to the stratigraphy of plate 6, but they could not accurately or consistently predict the locations of tailings beds in the subsurface. Subsurface tailings also occur disseminated within other sediment, principally gravel deposits. The following simple calculation illustrates one aspect of remediating subsurface tailings.

We developed an estimate of the volumes and weights of the two types of tailings (table 10). The volume of surficial tailings was estimated by assuming an average thickness of the beds. Although not exhaustive, our field observations of the tailings beds visible in the trench (pl. 6) and other exposures suggest that they are 0.3 m thick on average. Using that thickness and the extent of the beds visible in the 1997 photographs, the volume of the surficial tailings beds totals 16,000 m<sup>3</sup> (21,000 cubic yards). The greatest uncertainty in this estimate is our assumption of average thickness.

Estimating the volume of tailings in the subsurface is more complicated (table 10). We assumed that areas where gravel is presently exposed at the surface are areas where the stream aggraded or reworked the substrate in historical times, and thus are areas with tailings in the subsurface. The spatial extent of exposed gravel, including the active streambed, was estimated from the 1997 photographs (table 10). The gravel containing tailings is approximately 1 m thick at the trench, and we assume this thickness for all exposed gravel in reach B. The aggradation or depth of reworking in reaches C and D was likely less than in reach B, so we assumed a thickness of 0.5 m for all exposed gravel in those reaches. The limit to the accuracy of the results is probably these thickness assumptions. Accordingly the bulk volume of gravel containing tailings in the study area is on the order of 600,000 m<sup>3</sup> (780,000 cubic yards). Only a fraction of the gravel volume is tailings, however, so we assumed that 30 percent of the gravel deposits is sand and that two-thirds of the sand is tailings, which was derived in the section titled, "Geochemical Conclusions." In other words we assumed that 20 percent of the gravel volume is tailings. Accordingly the bulk volume of tailings in gravel of our study area is on the order of 120,000 m<sup>3</sup> (160,000 cubic yards). If the tailings in the subsurface were to be reclaimed, presumably the gravel would be sieved, separating the coarse clasts from the sand, and all of the sand would be hauled to a repository.

In conclusion, in order to reclaim the 120,000 m<sup>3</sup> of tailings, 600,000 m<sup>3</sup> of gravel would have to be excavated and sieved and 180,000 m<sup>3</sup> of material hauled to a repository. Reclaiming the 120,000 m<sup>3</sup> of coarse-grained tailings from the subsurface would thus be more involved than reclaiming the 16,000 m<sup>3</sup> of surficial beds of fine-grained tailings. The fine-grained tailings are also more susceptible to geochemical reactions, all other factors being equal, because the surface area (per unit mass) of the silty tailings is so much larger (perhaps 100 times larger) than that of the sandy coarse-grained tailings. On the other hand, the coarse-grained tailings are saturated by ground water for a large portion of the year, increasing the opportunity for geochemical reactions, whereas only rain and snowmelt wet the fine-grained tailings. It is beyond our expertise to evaluate the geochemical consequence of these differences in wetting times.

We estimated tailings volumes in order to also understand how much of the original tailings released still reside in the study area. The production of mill tailings was given in terms of weight, so the volume of tailings just discussed was converted to weight using a bulk density (table 10). Bulk density is the average density of mineral grains reduced by the volumetric proportion that is void space (porosity). The typical density of various minerals is given herein, in parentheses, in grams per cubic centimeter. The rocks of the watershed largely consist of volcanics of intermediate to silicic composition, which means that they are dominated by quartz (2.65) and feldspars ( $\approx$ 2.6) and a minor amount of mafic minerals (3.0–3.5). A fraction of the rocks are sulfides and other economic minerals that are fairly dense (3.5 to 5 and much greater). Thus the average density of bedrock may be close to 2.7 g/cm<sup>3</sup>. Because of the presence of tailings,

**Table 10.** Estimates of volumes and weights of tailings remaining in our study reach.

[Weights are expressed in metric tons (t)]

	Reach B	Reach C	Reach D	Total	Footnote
Surficial beds of fine-grained tailings					
Surface area, km <sup>2</sup>	0.030	0.018	0.005	0.053	1
Thickness, m	0.3	0.3	0.3	ng	2
Volume, m <sup>3</sup>	9,132	5,250	1,392	15,774	3
Volume, yd <sup>3</sup>	11,944	6,867	1,821	20,631	
Tailings weight, t	23,742	13,650	3,619	41,011	
Coarse tailings buried in gravel					
Surface area, km <sup>2</sup>	0.429	0.168	0.174	0.771	1
Thickness, m	1	0.5	0.5	ng	2
Gravel volume, m <sup>3</sup>	429,000	84,000	87,013	600,013	3
Gravel volume, yd <sup>3</sup>	561,111	109,868	113,809	784,787	
Sand volume, m <sup>3</sup>	128,700	25,200	26,104	180,004	4
Tailings volume, m <sup>3</sup>	84,942	16,632	17,229	118,803	5
Tailings volume, yd <sup>3</sup>	111,100	21,754	22,534	155,388	
Tailings weight, t	220,849	43,243	44,794	308,887	6
Fraction of total tailings produced					
Total weight, t	2,032,000				
Removed by streamflow	76 percent				
Reclaimed from reach B	12 percent				
Surface beds remaining	1 percent				
Within gravel remaining	11 percent				

<sup>1</sup>Estimated from 1997 aerial photographs.<sup>2</sup>Assumed based on field observations; ng, not given.<sup>3</sup>Bulk volume calculated as thickness times area.<sup>4</sup>Bulk volume of sand assumed to be 30 percent of gravel volume.<sup>5</sup>Bulk volume of tailings assumed to be 20 percent of gravel volume.<sup>6</sup>Assumes a bulk density of 2.6 g/cm<sup>3</sup>.

the dense minerals are more abundant in the sediment than they are in the bedrock. We assume an average mineral density of 3.5 g/cm<sup>3</sup> for the fine sediment containing tailings. We also assume a porosity of 25 percent, which yields a sediment bulk density of 2.6 g/cm<sup>3</sup>. The results are given in table 10. Of the original tailings produced, the majority, perhaps 70–80 percent, has been flushed from the study reach by streamflow. The owners of the Sunnyside mine had “120,000 cubic yards” of tailings mechanically removed from reach B in 1997 (Rob Robinson, Bureau of Land Management, written commun., 2004), which constitutes a significant fraction, perhaps 10 percent, of the amount produced. The tailings remaining in the study area are also a fraction of the original, on the order of 12 percent, but are substantial in terms of their volume and weight (table 10). Of that remaining in the landscape, on the order of 10 percent exists at the surface as identifiable and accessible tailings beds, and the majority is in the subsurface dispersed within gravel deposits.

## Summary and Conclusions

In this study we document the physical nature of the upper Animas River and its flood plain in several study reaches between Eureka and Howardsville (figs. 1, 3, 4), during the latest Holocene and in detail during the past century. The Animas River was likely never a classical (narrow, deep, tree-shaded, and single-threaded) meandering stream, based on comparison with meandering and braided streams in general (fig. 5). In addition, a sediment transport calculation indicated that a hypothetical single-threaded channel would be unstable: it would locally fill with gravel and thus force braiding to occur. This is the result of the strongly concave shape of the longitudinal profile in reaches A and B (fig. 3), which causes boundary shear stress (fig. 6), and thus bed load transport rates, to decrease rapidly downstream. Spatial variation in bed load transport rates causes local erosion and

deposition that will persist until the channel morphology adjusts to remove the uneven transport rates. Given a strongly concave valley profile, the end result of uniform bed load transport down the Animas River inevitably involves a spatial transition of channel shape down the valley. Prior to the activities of miners, this involved a transition from a braided stream in reach A to multi-threaded channels at the downstream end of reach B. The channels transitioned from being braided (multiple shallow channels with largely indistinct banks) to what we call multi-threaded: more than one relatively stable channel with most having steep and relatively high banks. A century ago, reach A consisted of a braided and shifting channel (figs. 8 and 9A). Reach A is upstream of Eureka and thus upstream of the source of tailings from the mills associated with the Sunnyside mine.

The sediment transport model suggests that reach B is inherently susceptible to braiding, and other evidence demonstrates that the Animas River in reach B was alternately braided and multi-threaded during periods of the late Holocene. Extensive gravel deposits dominate the base of the stratigraphic section exposed in the trench (pl. 6). We interpreted this to represent a period of deposition and reworking by broad braided streams, with only localized deposition (or preservation) of fine-grained flood-plain deposits. This period apparently ended about a thousand years ago (fig. 13). After that, the brown silt flood-plain deposits began to accumulate (and were preserved) in between multiple channels of the Animas River at the trench site. The banks of these channels were on the order of 1 m high. The flood plain likely consisted of dense thickets of willow and areas of grasses between sparse willow bushes. Thin layers of peat within the silt beds suggest that beaver ponds were locally or occasionally present on the flood plain. This period of multi-threaded channels surrounded by vegetated flood plain persisted until the early 20th century, based on the observations made from early historical photographs. The multi-threaded channels evident in the ca 1904 photograph (fig. 2A), in particular, support the stratigraphic interpretation of the nature of channels and flood plain. The persistence of that channel configuration for perhaps a thousand years demonstrates a geomorphic equilibrium involving uniform bed load transport. This equilibrium condition ended abruptly. The stratigraphy (pl. 6) reveals that dramatic and rapid changes in the upper Animas River valley occurred during historical times. At least at the trench site, the channels were filled with gravel, after which the Animas River reverted to a braided condition and broad sheets of gravel were deposited over the formerly vegetated flood plain. The upper end of reach B also apparently aggraded, as that would explain the current absence of 1-m high banks that are evident in that area in the 1883–84 photograph, and which are faintly visible in the 1904 photograph (fig. 2A). Subsequently, beds of fine-grained tailings were deposited over much of the valley floor of reach B (fig. 4).

The timing of this episode of dramatic channel change is fairly tightly constrained. Coarse-grained tailings are locally found at the base of buried channels (pl. 6) and may have been deposited late in the 19th century or early in the 20th century.

This deposition likely occurred after 1900, however. Only a modest quantity of tailings was produced before 1900 (fig. 7); and after 1900, coarse-grained tailings were produced in quantity directly adjacent to the Animas River at the head of reach B. Channels in reach B were not full of gravel in 1904 (fig. 2A). The channels may have been partially filled with gravel during the 1911 flood, which is the flood of record. At the site of the dated willows (fig. 12), 100 m downstream of the trench, gravel at the base of the section was likely deposited in 1911, but the bulk of the streambed gravel at that site was probably deposited during the 1921 and 1927 floods. Much of the gravel accumulation in the reach at the trench also likely occurred in the 1920s. In the aerial photographs (fig. 4), the fine-grained tailings appear to have been purposely placed behind the gravel berms in reach B, and tailings stopped being produced in quantity in 1930. Thus channel aggradation may have ceased before 1930. In the field we observed large areas of ground surface consisting of blackened gravel or tailings beds at the trench site, and these features are evident in the 1945 aerial photograph. Thus, at the latest, the period of rapid aggradation ended before 1945.

Why did the channels in reach B aggrade? The first argument involves a coincidence in space and in time. The Animas River underwent a dramatic change from a stable geomorphic condition and transformed into a braided reach that is unique in the region. Mining activities (but not milling) were extensive in the Cement Creek basin, for example, but Cement Creek did not experience dramatic physical changes during historical times (Vincent and others, this volume). The unique reach B is located immediately downstream of mills that produced between 35,000 and 330,000 metric tons per year of tailings. Furthermore, the channels began to fill immediately after the period when mills supplied large quantities of sand-sized tailings directly to the fluvial system. This argument suggests that tailings played an important role in causing channel change.

Understanding the causal mechanism is tricky, however, and two issues must be explained. The first issue is the source of the gravel clasts filling the paleochannels of reach B (pl. 6). This is important, because the bulk of the gravel consists of subrounded stream-gravel clasts, unrelated to mining or milling. We believe that these clasts were derived from the substantial deposits in reach A, in part because the Animas River in reach A appears to have incised after 1906 (fig. 9). The second issue involves our explaining how the delicately balanced condition of uniform bed load transport through reach B became altered. We do not think that the fine-grained tailings played the major role. On the one hand, the tailings beds may have acted to increase the heights of banks, locally allowing flows to be deeper and exert higher boundary shear stress, resulting in anomalously high bed load transport rates. On the other hand, however, the beds of fine-grained tailings are dominated by silt, and field evidence (climbing ripples) demonstrated that silt was carried in suspension. As suspended load, silt could influence bed load transport by decreasing the

fluid viscosity and decreasing the density contrast of the fluid and bed material. Suspended sediment rarely makes up even 5 percent of the fluid volume, however, and we do not think that the influence on bed load transport is sufficiently strong to cause the observed changes. We suspect the sand-sized tailings altered bed load transport in the following way. Suspended transport of sand cannot be supported unless patches of sand are present on the bed, which essentially makes the bed smoother, effectively lowering the critical shear stress for transport of pebbles on the bed.

We offer the following sequence of events as a hypothesis. After 1900 sand-sized tailings were produced in abundance but largely resided near the mill until a major flood occurred. A major flood occurred in 1911, depositing tailings from this site in the Animas River canyon (Church, Fey, and Unruh, this volume, fig. 20). This flood mobilized gravel in reach A, but when the gravel encountered the abundant sand near the mills the sediment transport rate increased, perhaps causing local incision in the upper portion of reach B. As the excessive bed load encountered the decreasing gradient of the middle and lower portions of reach B, the transport rate decreased and gravel was deposited in the multi-threaded channels, but did not fill them. Sand-sized tailings continued to be produced until at least 1913, if we interpret the discussion by Jones (this volume) of the "Gravity Milling era" correctly. Alternatively, sand-sized tailings may have continued to be produced in abundance until the efficient Sunnyside Eureka Mill was completed in 1918. In any case the sand largely resided near the mill(s) until a large flood occurred. A large flood did occur in 1921, and an even larger flood occurred in 1927; and just as in 1911, gravel was removed from reach A and deposited in the lower portion of reach B, with one change occurring. As sediment was deposited in the channels at the downstream end of reach B, the gradient of the reach was reduced. The reduced gradient, and shallowing of the flow due to braiding, caused the locus of deposition to migrate upstream until all channels in reach B were filled. The original gradient was thus restored and uniform bed load transport resumed, just as our calculations suggest that transport is currently uniform in the subreach containing the surveyed cross sections at the downstream end of reach B. In any case aggradation did occur in reach B, whereas changes in reaches C and D, which have more uniform profile gradients, were comparatively minor.

Tailings became disseminated within streambed gravel in the subsurface (pl. 6) during aggradation, and are also found as easily identifiable beds at the ground surface (fig. 11). As a direct result of the presence of tailings, the concentrations of zinc (fig. 14) and other metals (table 8) are dramatically elevated compared to those of prehistorical sediment, whereas vanadium and other elements are more dilute. Streamflows have been reworking the tailings (table 9), and have transported between 70 and 80 percent of the tailings originally produced out of our study area (table 10). Of the tailings that remain in our study area, on the order of 10 percent exists as distinct beds of fine-grained tailings at the ground surface (table 10). If the assumptions of our calculations are correct,

the majority (90 percent) is located in the shallow subsurface, and consists of predominantly sand-sized tailings particles mixed with gravel. It is our understanding that the environmental concern over tailings is that "water/rock" geochemical reactions will liberate metals from tailings particles and increase metal concentrations in ground water and (or) surface water. The concentrations of metals are similar in the two types of tailings (table 8), with the exception of lead, and manganese to a lesser degree, which have higher concentrations in the fine-grained tailings. Thus, the two deposit types are similar in that way. Yet, there are important differences in the two types of tailings deposits. It is our understanding that the rates of geochemical reaction with solid particles are directly proportional to the surface areas of those particles, all other factors being the same. The fine-grained tailings have about 100 times more surface area (per unit mass) compared to the coarse-grained tailings. It is also our understanding that the efficacy of geochemical reactions increases with increasing duration of the contact of water and solid particles. We presume that the duration of contact with water is greater for the coarse-grained tailings, as they are located in the subsurface and are presumably in contact with ground water for a large portion of the year. Thus, the rates of geochemical reactions of water with coarse-grained tailings may be relatively slow (per unit time), yet the coarse-grained tailings are far more abundant and the duration of their contact with water is longer, compared with that for the fine-grained tailings. On the other hand, the fine-grained tailings are susceptible to being mobilized by streamflow (but, at present, likely only by large floods), and being exported to areas outside of our study area where they may cause problems. The coarse-grained tailings are comparatively protected in the subsurface from mobilization by streamflow. It is beyond our expertise to balance these different factors and judge the relative environmental impact of the two tailings types, but we hope that the information that we have provided will enable others to do so.

## References Cited

- Andrews, E.D., 1983, Entrainment of gravel from naturally sorted riverbed material: Geological Society of America Bulletin, v. 94, p. 1225–1231.
- Andrews, E.D., and Smith, J.D., 1992, A theoretical model for calculating marginal bedload transport rates of gravel, *in* Billi, P., Hey, R.D., Thorne, C.R., and Tocconi, P., eds., Dynamics of gravel-bed rivers: New York, John Wiley, p. 41–52.
- Atwood, W.W., and Mather, K.F., 1932, Physiography and Quaternary geology of the San Juan Mountains, Colorado: U.S. Geological Survey Professional Paper 166, 176 p.
- Begin, Z.B., 1981, The relationship between flow-shear stress and stream pattern: Journal of Hydrology, v. 52, p. 307–319.

- Birkeland, P.W., 1984, *Soils and geomorphology*: New York, Oxford, 372 p.
- Bird, A.G., 1986, *Silverton gold—The story of Colorado's largest gold mine*: Lakewood, Colo., privately published (ISBN 0-9619382-2-6), 152 p.
- Blair, R.W., Jr., Yager, D.B., and Church, S.E., 2002, *Surficial geologic maps along the riparian zone of the Animas River and its headwater tributaries, Silverton to Durango, Colorado, with upper Animas River gradient profiles*: U.S. Geological Survey Digital Data Series DDS-71, one CD-ROM.
- Briggs, P.H., 1996, Forty elements by inductively coupled plasma-atomic emission spectrometry, *in* Arbogast, B.F., ed., *Analytical methods manual for the Mineral Resources Program*: U.S. Geological Survey Open-File Report 96-525, p. 77-94.
- Campbell, D.L., and Eckhart, L.C., 2000, *Geoelectrical studies of a trenched line across the Animas River, San Juan County, Colorado*: U.S. Geological Survey Open-File Report 00-112, 92 p., 114 leaves.
- Carrara, P.E., Trimble, D.A., and Rubin, Meyer, 1991, Holocene treeline fluctuations in the northern San Juan Mountains, Colorado, U.S.A., as indicated by radiocarbon-dated conifer wood: *Arctic and Alpine Research*, v. 23, p. 233-246.
- Carson, M.A., 1984, The meandering-braided river threshold—A reappraisal: *Journal of Hydrology*, v. 73, p. 315-334.
- Dunne, Thomas, and Leopold, L.B., 1978, *Water in environmental planning*: San Francisco, Freeman, 818 p.
- Durango Evening Herald, 1911, Oct. 5-11 editions, Durango, Colo.
- Elliott, J.G., and Gyetvai, Steven, 1999, Channel-pattern adjustments and geomorphic characteristics of Elkhead Creek, Colorado, 1937-97: U.S. Geological Survey Water-Resources Investigations Report 99-4098, 39 p.
- Elliott, J.G., and Hammack, L.A., 2000, Entrainment of riparian gravel and cobbles in an alluvial reach of a regulated canyon river: *Regulated Rivers—Research and Management*, v. 16, no. 1, p. 37-50.
- Emsley, John, 1991, *The elements*: Oxford, Clarendon Press, 251 p.
- Environmental Systems Research Institute, Inc., 1996, *ArcView spatial analyst user's manual*: Redlands, Calif., ESRI Press, 147 p.
- Fey, D.L., Church, S.E., and Unruh, D.M., 2000, *Geochemical and lead isotopic data from sediment cores, fluvial tailings, iron bogs, and premining terrace deposits, Animas River watershed, Colorado, 1995-1999*: U.S. Geological Survey Open-File Report 00-465, 91 p.
- Graf, W.H., 1971, *Hydraulics of sediment transport*: New York, McGraw-Hill, 513 p.
- Gurnell, A.M., 1997, Channel change on the River Dee meanders, 1946-1992, from the analysis of air photographs: *Regulated Rivers—Research and Management*, v. 13, p. 13-26.
- Hastings, J.R., and Turner, R.M., 1965, *The changing mile—An ecological study of vegetation change with time in the lower mile of an arid and semiarid region*: Tucson, Ariz., University of Arizona Press, 317 p.
- Henderson, F.M., 1966, *Open channel flow*: New York, Macmillan, 522 p.
- Jensen, J.R., 1996, *Introductory digital image processing—A remote sensing perspective*: Upper Saddle River, N.J., Prentice Hall, 316 p.
- Kean, J.W., and Smith, J.D., 2004, Flow and boundary shear stress in channels with woody bank vegetation, *in* Bennett, S.J., and Simon, Andrew, eds., *Riparian vegetation and fluvial geomorphology*: American Geophysical Union, *Water Science and Application* 8, p. 237-252.
- King, W.H., and Allsman, P.T., 1950, *Reconnaissance of metal mining in the San Juan region, Ouray, San Juan, and San Miguel Counties, Colorado*: U.S. Bureau of Mines Information Circular 7554, 109 p.
- Komar, P.D., 1987, Selective gravel entrainment and the empirical evaluation of flow competence: *Sedimentology*, v. 34, p. 1165-1176.
- Leopold, L.B., and Miller, J.P., 1956, *Ephemeral streams—Hydraulic factors and their relation to the drainage net*: U.S. Geological Survey Professional Paper 282-A, p. 1-37.
- Leopold, L.B., and Wolman, M.G., 1957, *River channel patterns—Braided, meandering and straight*: U.S. Geological Survey Professional Paper 282-B, p. 39-84.
- Lisle, T.E., Iseya, F., and Ikeda, H., 1993, Response of a channel with alternate bars to a decrease in supply of mixed-size bed load—A flume experiment: *Water Resources Research*, v. 29, p. 3623-3629.
- Malde, H.E., 1973, *Geologic bench marks by terrestrial photography*: U.S. Geological Survey *Journal of Research*, v. 1, p. 193-206.

- Marshall, J., 1996, Mining the hard rock in the Silverton San Juans: Silverton, Colo., Simpler Way Book Company, 216 p.
- Meyer-Peter, E., and Müller, R., 1948, Formulas for bed-load transport: Proceedings of the Second Meeting of the International Association of Hydraulic Research, Stockholm, Sweden, p. 39–64.
- Middleton, G.V., and Southard, J.B., 1984, Mechanics of sediment movement: Society of Economic Paleontologists and Mineralogists, SEPM Short Course 3, 401 p.
- Milhou, R.T., 1982, Effect of sediment transport and flow regulation on the ecology of gravel-bed rivers, *in* Hey, R.D., Bathurst, J.C., and Thorne, C.R., eds., Gravel-bed rivers: Chichester, England, John Wiley, p. 819–842.
- Munsell Color, 2000, Munsell soil color charts: New Windsor, N.Y., GretagMacbeth, pages variable.
- National Institute of Standards and Technology (NIST), 1993a, Certificate of analysis standard reference material 2704, Buffalo River sediment.
- National Institute of Standards and Technology (NIST), 1993b, Certificate of analysis standard reference material 2709, San Joaquin soil.
- National Institute of Standards and Technology (NIST), 1993c, Certificate of analysis standard reference material 2711, Montana soil.
- Neill, C.R., 1968, A re-examination of the beginning of movement for coarse granular bed materials: Wallingford, U.K., Hydraulics Research Station, Report INT 68, 37 p.
- Osterkamp, W.R., 1978, Gradient, discharge and particle-size relations of alluvial channels in Kansas, with observations on braiding: American Journal of Science, v. 278, p. 1253–1268.
- Ostroff, Eugene, 1981, Western views and eastern visions: Smithsonian Institution Traveling Exhibition Service, U.S. Government Printing Office, 116 p.
- Parker, Gary, Klingman, P.C., and McLean, D.G., 1982, Bedload and size distribution in paved gravel-bed streams: American Society of Civil Engineers, Journal of the Hydraulics Division, v. 108, no. HY4, p. 544–571.
- Pruess, J.W., 1996, Paleoflood reconstructions within the Animas River basin upstream from Durango, Colorado: Fort Collins, Colo., Colorado State University M.S. thesis, 192 p.
- Richards, Keith, 1982, Rivers—Form and process in alluvial channels: London, Methuen, 358 p.
- Rogers, G.F., Malde, H.E., and Turner, R.M., 1984, Bibliography of repeat photography for evaluating landscape change: Salt Lake City, Utah, University of Utah Press, 215 p.
- Schumm, S.A., and Khan, H.R., 1972, Experimental study of channel patterns: Geological Society of America Bulletin, v. 83, p. 1755–1770.
- Scott, M.L., Auble, G.T., and Friedman, J.M., 1997, Flood dependency of cottonwood establishment along the Missouri River, Montana, U.S.A.: Ecological Applications, v. 7, p. 677–690.
- Shields, A., 1936, Anwendung der ahnlichkeitsmechanik und der turbulenzforschung auf die Geschiebebewegung [Application of similarity principles and turbulence research to bedload movement]: Berlin, Mitteilung Preussischen Versuchanstalt für Wasserbau und Schiffbau, Report 26, 24 p. [See translation by Ott, W.P., and von Uchelen, J.C.: Pasadena, Calif., California Institute of Technology Hydrodynamics Report 167, 43 p.]
- Sigafoos, R.S., 1964, Botanical evidence of floods and flood-plain deposition: U.S. Geological Survey Professional Paper 485-A, 35 p.
- Silverton Standard, 1904, San Juan County: Silverton Standard, Silverton, Colorado, 28 p.
- Sloan, R.E., and Skowronski, C.A., 1975, The rainbow route: Denver, Colo., Sundance Publications Limited, 416 p.
- Smith, J.D., 2004, The role of riparian shrubs in preventing floodplain unraveling along the Clark Fork of the Columbia River in the Deer Lodge Valley, Montana, *in* Bennett, S.J., and Simon, Andrew, eds., Riparian vegetation and fluvial geomorphology: American Geophysical Union, Water Science and Application 8, p. 71–85.
- Smith, J.D., and Griffin, E.R., 2002, Relation between geomorphic stability and the density of large shrubs on the flood plain of the Clark Fork of the Columbia River in the Deer Lodge Valley, Montana: U.S. Geological Survey Water-Resources Investigations Report 02–4070, 25 p.
- Stuiver, Minze, and Braziunas, T.F., 1993, Sun, ocean, climate and atmospheric  $^{14}\text{CO}_2$ —An evaluation of causal and spectral relationships: The Holocene, v. 3, no. 4, p. 289–305.
- Stuiver, Minze, and Reimer, P.J., 1993, Extended  $^{14}\text{C}$  data base and revised CALIB 3.0  $^{14}\text{C}$  age calibration program: Radiocarbon, v. 35, p. 215–230.
- Stuiver, Minze, Reimer, P.J., Bard, Edouard, Beck, J.W., Burr, G.S., Hughen, K.A., Kromer, Bernd, McCormac, Gerry, van der Plicht, Johannes, and Spurk, Marco, 1998, INTCAL98 radiocarbon age calibration, 24,000–0 cal BP: Radiocarbon, v. 40, p. 1041–1083.

- Thode, J.C., 1989, George L. Beam and the Denver and Rio Grande, Volume II: Denver, Colo., Sundance Publications, 280 p.
- Thorne, C.R., 1990, Effects of vegetation on riverbank erosion and stability, *in* Thornes, J.B., ed., *Vegetation and erosion*: New York, John Wiley, p. 125–144.
- U.S. Interagency Advisory Committee on Water Data, 1982, Guidelines for determining flood-flow frequency: Reston, Va., Bulletin 17B of the Hydrology Subcommittee, U.S. Geological Survey, Office of Water Data Coordination, 183 p.
- Vincent, K.R., Church, S.E., and Fey, D.L., 1999, Geomorphological context of metal-laden sediments in the Animas River floodplain, Colorado, *in* Morganwalp, D.W., and Buxton, H.T., eds., *U.S. Geological Survey Toxic Substances Hydrology Program—Proceedings of the Technical Meeting, Charleston, South Carolina, March 8–12, 1999, Volume 1 [of 3]—Contamination from hardrock mining*: U.S. Geological Survey Water-Resources Investigations Report 99–4018A, p. 99–106.
- Whiting, P.J., and Dietrich, W.E., 1989, The roughness of alluvial surfaces; an empirical examination of the influence of size heterogeneity and natural packing: *Eos*, v. 70, no. 43, p. 1109.
- Wiberg, P.L., and Smith, J.D., 1987, Calculations of the critical shear stress for motion of uniform and heterogeneous sediments: *Water Resources Research*, v. 23, p. 1471–1480.
- Wiberg, P.L., and Smith, J.D., 1991, Velocity distribution and bed roughness in high-gradient streams: *Water Resources Research*, v. 27, no. 5, p. 825–838.
- Wilcock, P.R., 1992, Flow competence—A criticism of a classic concept: *Earth Surface Processes and Landforms*, v. 17, p. 289–298.
- Wilcock, P.R., and McArdell, B.W., 1993, Surface-based fractional transport rates—Mobilization thresholds and partial transport of a sand-gravel sediment: *Water Resources Research*, v. 29, p. 1297–1312.
- Wolman, M.G., 1954, A method of sampling coarse river-bed material: *American Geophysical Union Transactions*, v. 35, p. 951–956.

